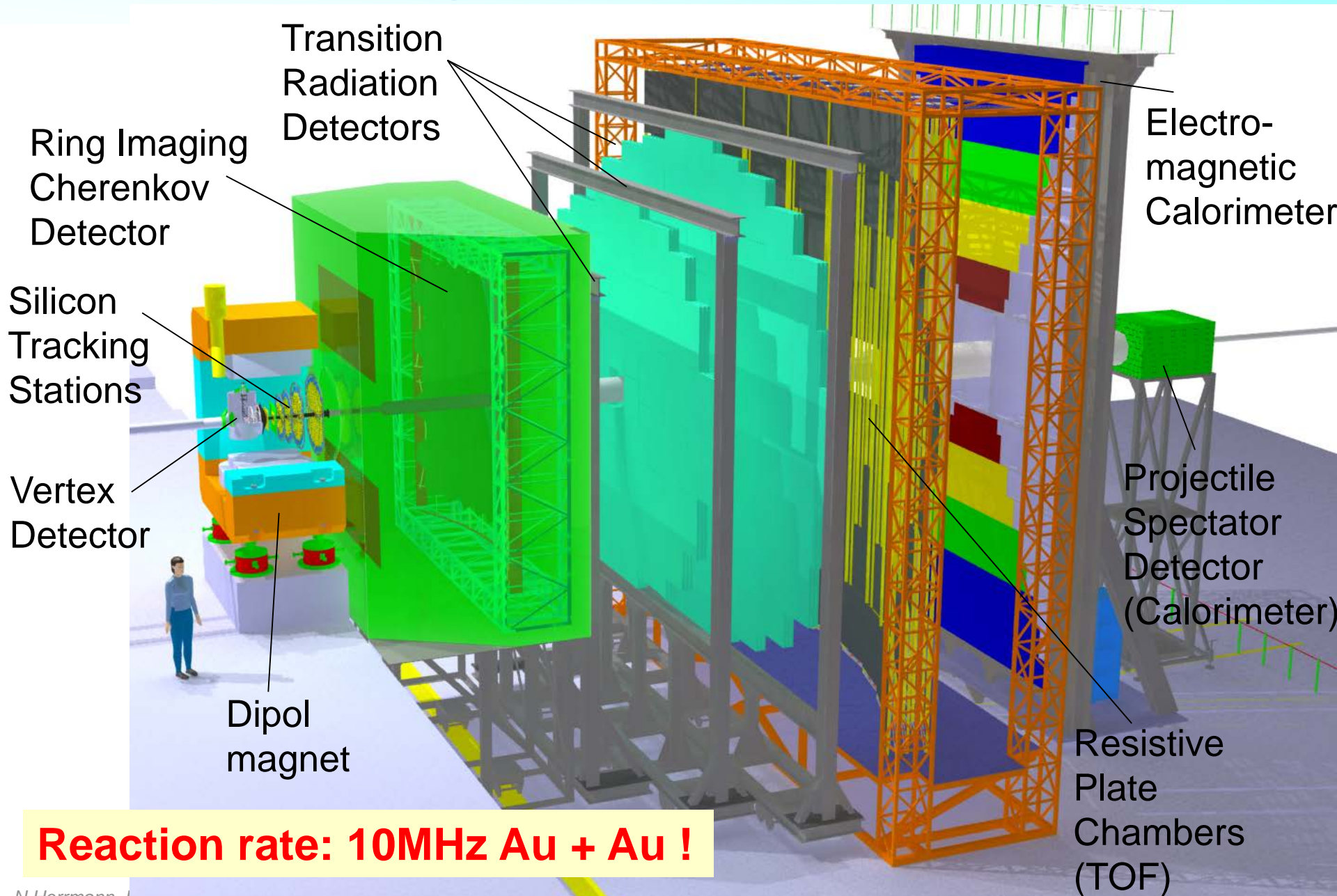




9th Terascale Detector Workshop

Introduction on Timing

Background: CBM @ FAIR



Outline

History

Timing applications

Timing counter types

Plastic scintillator

MRPC counter

Diamond beam counter

Nobelprize in Physics 1954



"for the coincidence method and his discoveries made therewith"

Walter Bothe



born 1891
died 1957

1908 – 12	Study of Physics at the University of Berlin
1913 – 29	Physikalisch – Technische Reichsanstalt, Berlin
1929	Extraordinary Professor, Berlin
1930 – 32	Professor of Physics, Giessen
1933 – 57	Director of the Institute of Physics and Max Planck Institute for Medical Research, Heidelberg

First coincidence circuit

Detector 1

Detector 2

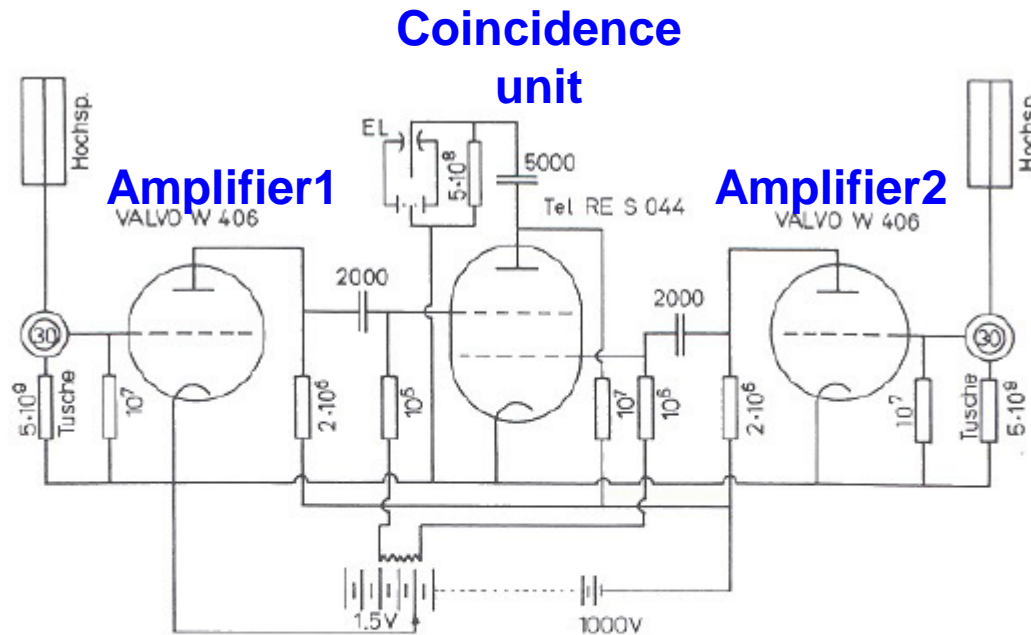


Abb.2. Erste Koinzidenzschaltung Bothes (1928). Von einer Freihandskizze in Bothes Protokollbuch abgezeichnet. EL: Einfadenelektrometer RES 044 (S = Schutzgitter; 004 = 4 Volt Heizspannung) W 406 (W = Niederfrequenzradiatorröhre für Widerstandskopplung) 406 = 4 Volt Heizspannung, 0,06 Amp Heizstrom)

Timing resolution: $\Delta t \approx 0.1 \text{ ms}$

Timing applications in Nuclear and Particle Physics

Event definition

Particle Identification

Direction measurement

Cosmic air showers,

Cerenkov cone of charged particle in neutrino detectors

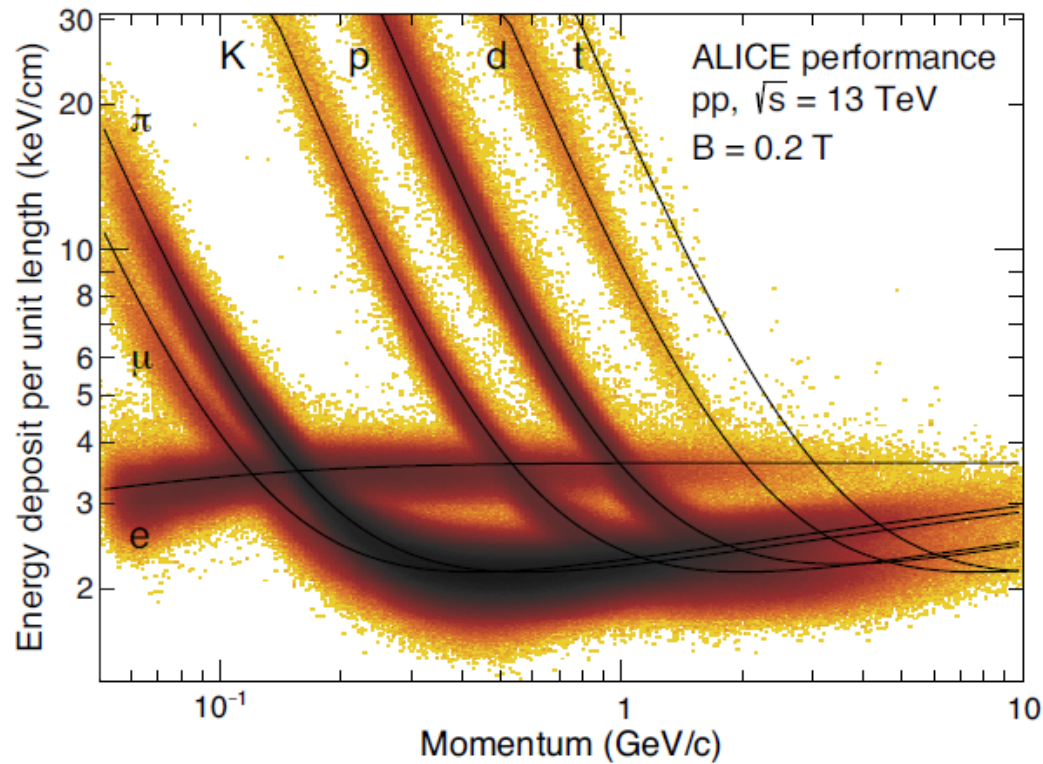
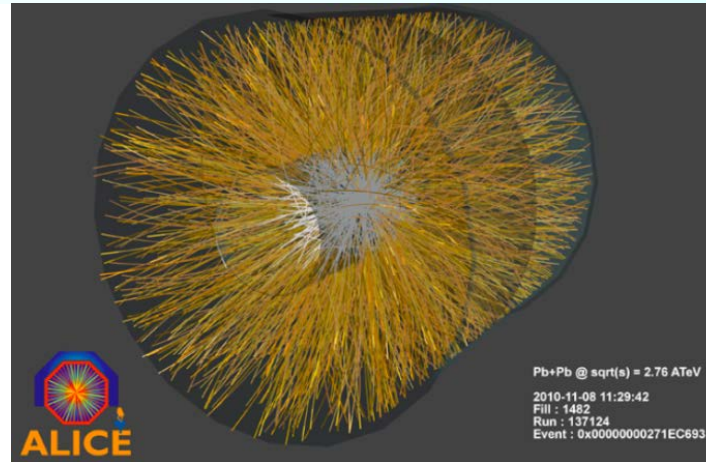
TOF – PET

T0 – measurements of particle beams

Spectroscopy in Neutron scattering

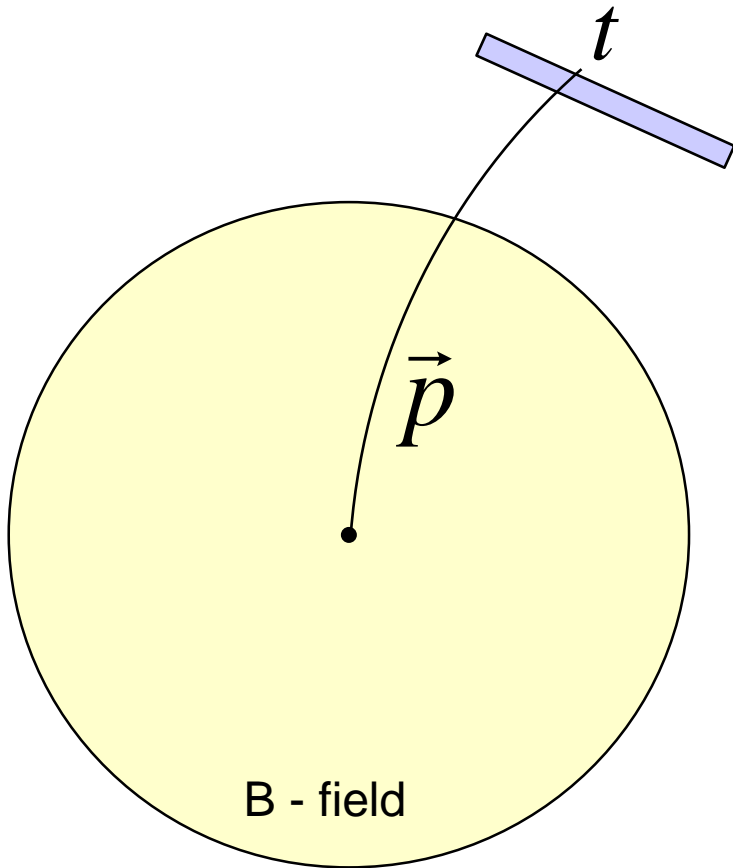
...

Particle identification (PID)



Time – of – Flight Method

Typical Setup



Tracking in magnetic field measures momentum.

Additional measurement of velocity allows determination of particle mass.

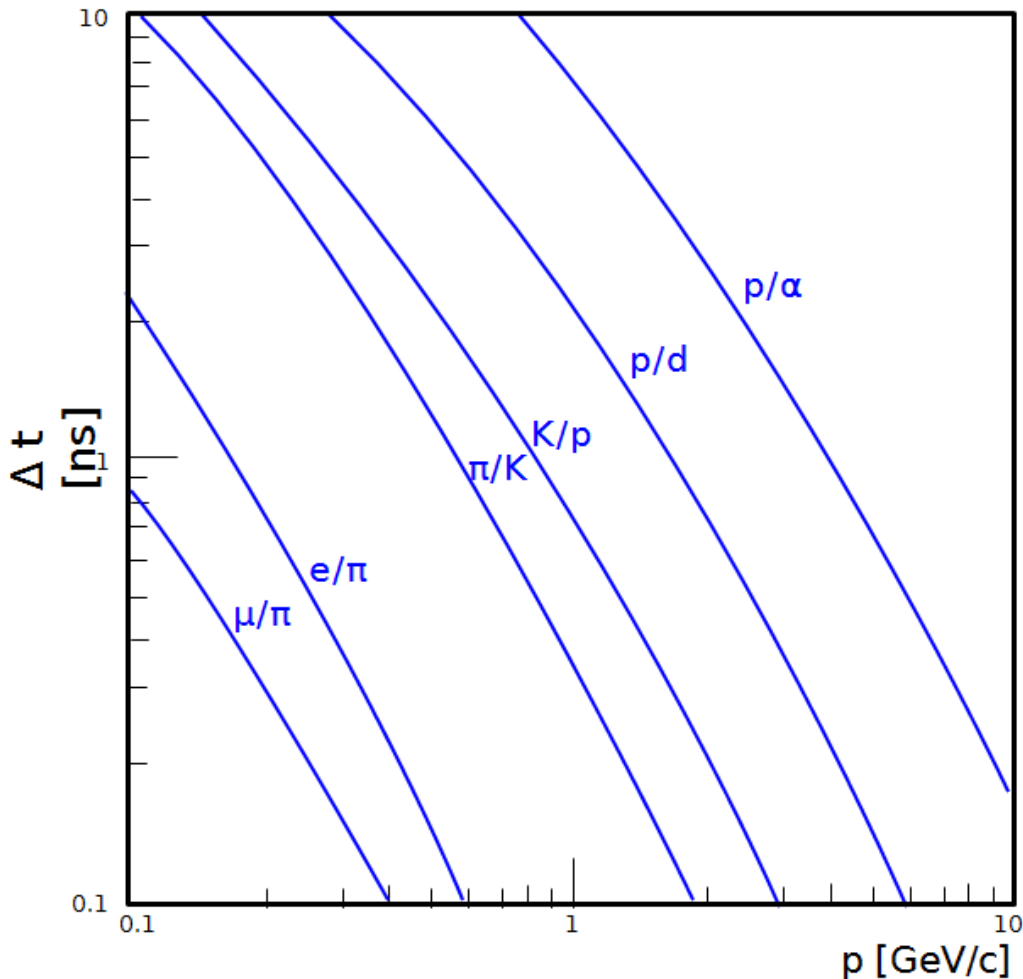
$$\beta = \frac{L}{ct}$$

$$p = mc\gamma\beta = \frac{mc\beta}{\sqrt{1-\beta^2}}$$

$$m^2 = \left(\frac{p}{c}\right)^2 \left(\frac{1}{\beta^2} - 1\right) = \left(\frac{p}{c}\right)^2 \left(\frac{c^2 t^2}{L^2} - 1\right)$$

PID reach with TOF

Flight Time difference after a pathlength of 1 m



$$\Delta t = \frac{L}{c} \left(\sqrt{\frac{m_1^2 c^2}{p^2} + 1} - \sqrt{\frac{m_2^2 c^2}{p^2} + 1} \right)$$

$$\downarrow pc \gg mc^2$$

$$\approx \frac{Lc}{2p^2} (m_1^2 - m_2^2)$$

TOF system time resolution requirement:

$$\Delta t > k\sigma_t$$

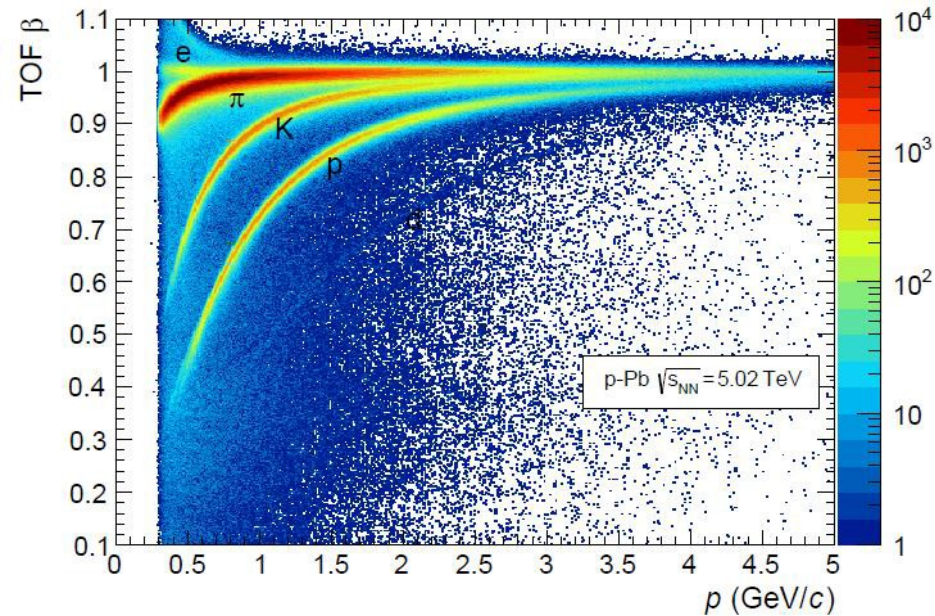
$$k > 3-4$$

(depends on relative abundance)

PID with TOF

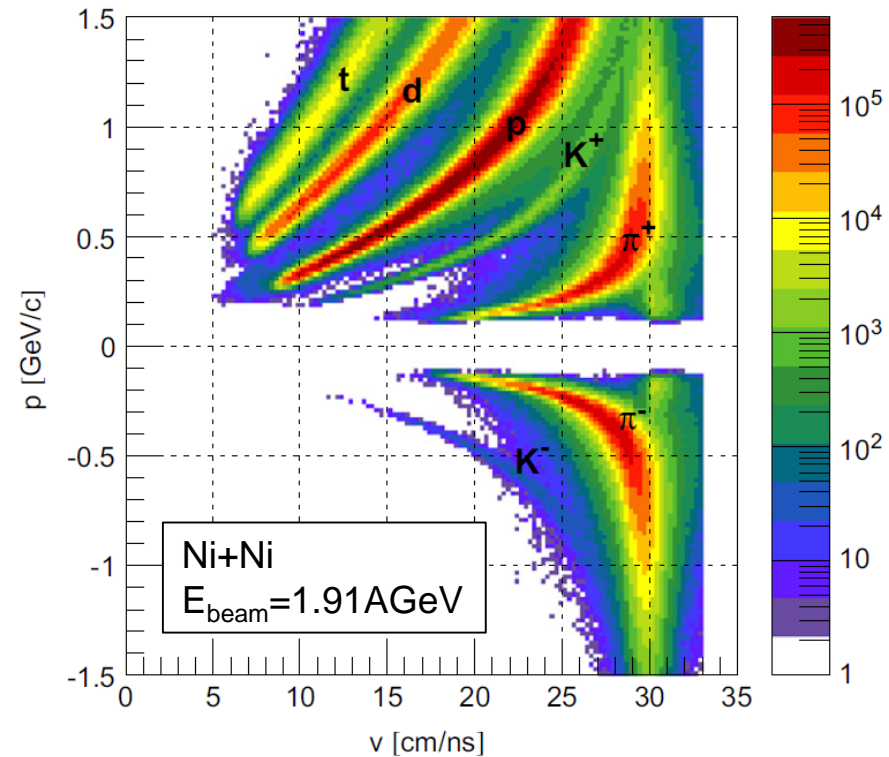


A. Akindinov et al. (ALICE), EPJ Plus 128 (2013) 44



L ~ 4 m

M. Kis et al. (FOPI), NIM A 646, 27 (2011)



L ~ 1.2 m

TOF mass resolution

Here: $c=1$

$$m^2 = p^2 \left(\frac{t^2}{L^2} - 1 \right)$$

$$\delta(m^2) = 2p\delta p \underbrace{\left(\frac{t^2}{L^2} - 1 \right)}_{\frac{m^2}{p^2}} + \underbrace{2t\delta t \frac{p^2}{L^2} - 2\frac{\delta L}{L^3} p^2 t^2}_{\text{use } \frac{p^2 t^2}{L^2} = \frac{p^2}{\beta^2} = m^2 \gamma^2}$$

$$= 2m^2 \frac{\delta p}{p} + 2m^2 \gamma^2 \frac{\delta t}{t} - 2m^2 \gamma^2 \frac{\delta L}{L}$$

⇓

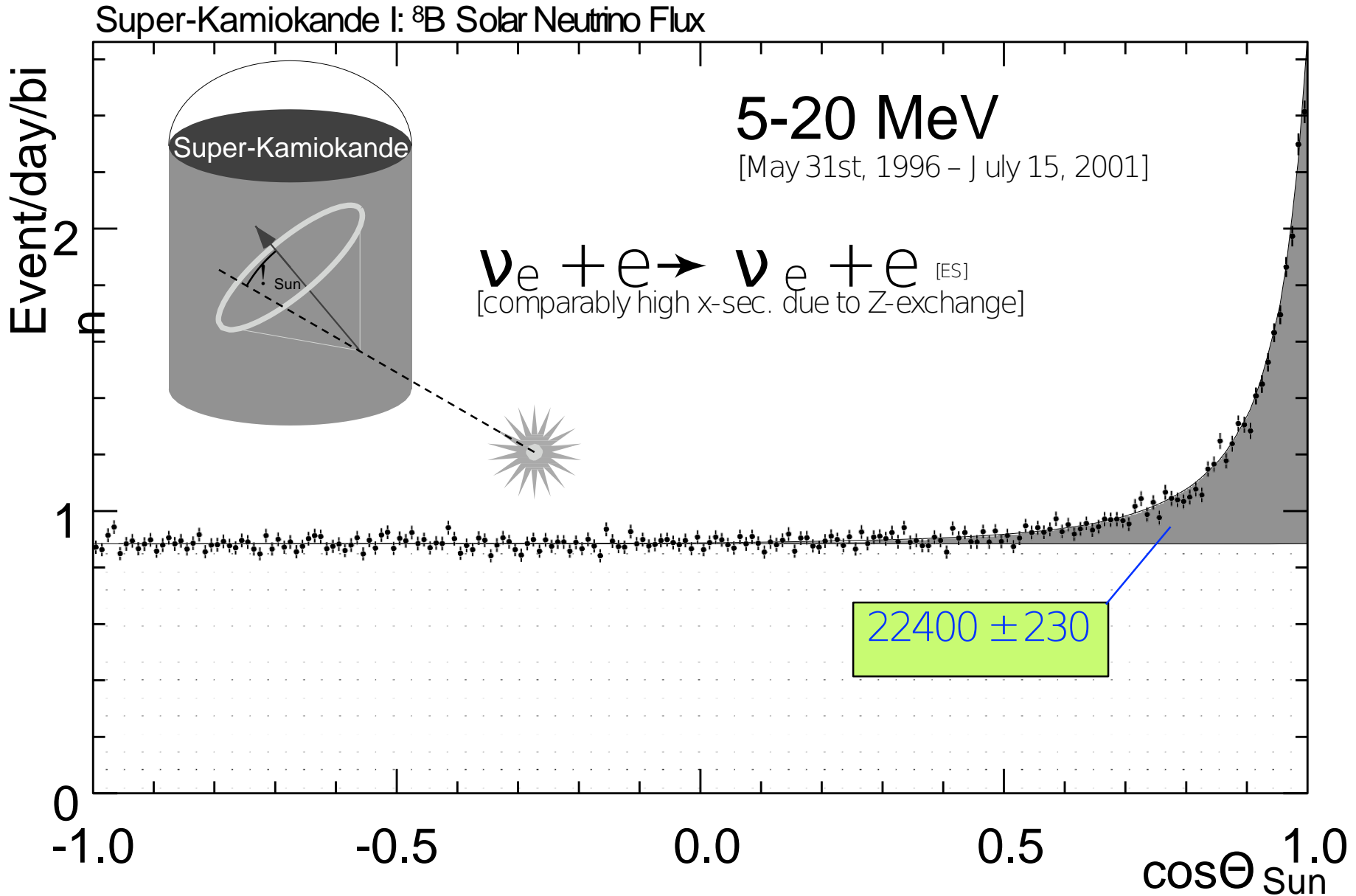
$$\left(\frac{\sigma_m}{m} \right)^2 = 4m^2 \left(\left(\frac{\sigma_p}{p} \right)^2 + \gamma^4 \left(\left(\frac{\sigma_t}{t} \right)^2 + \left(\frac{\sigma_L}{L} \right)^2 \right) \right)$$

Typical values:

$$\frac{\sigma_p}{p} \approx 10^{-2}, \quad \frac{\sigma_t}{t} \approx 10^{-1}, \quad \frac{\sigma_L}{L} \approx 10^{-3}$$

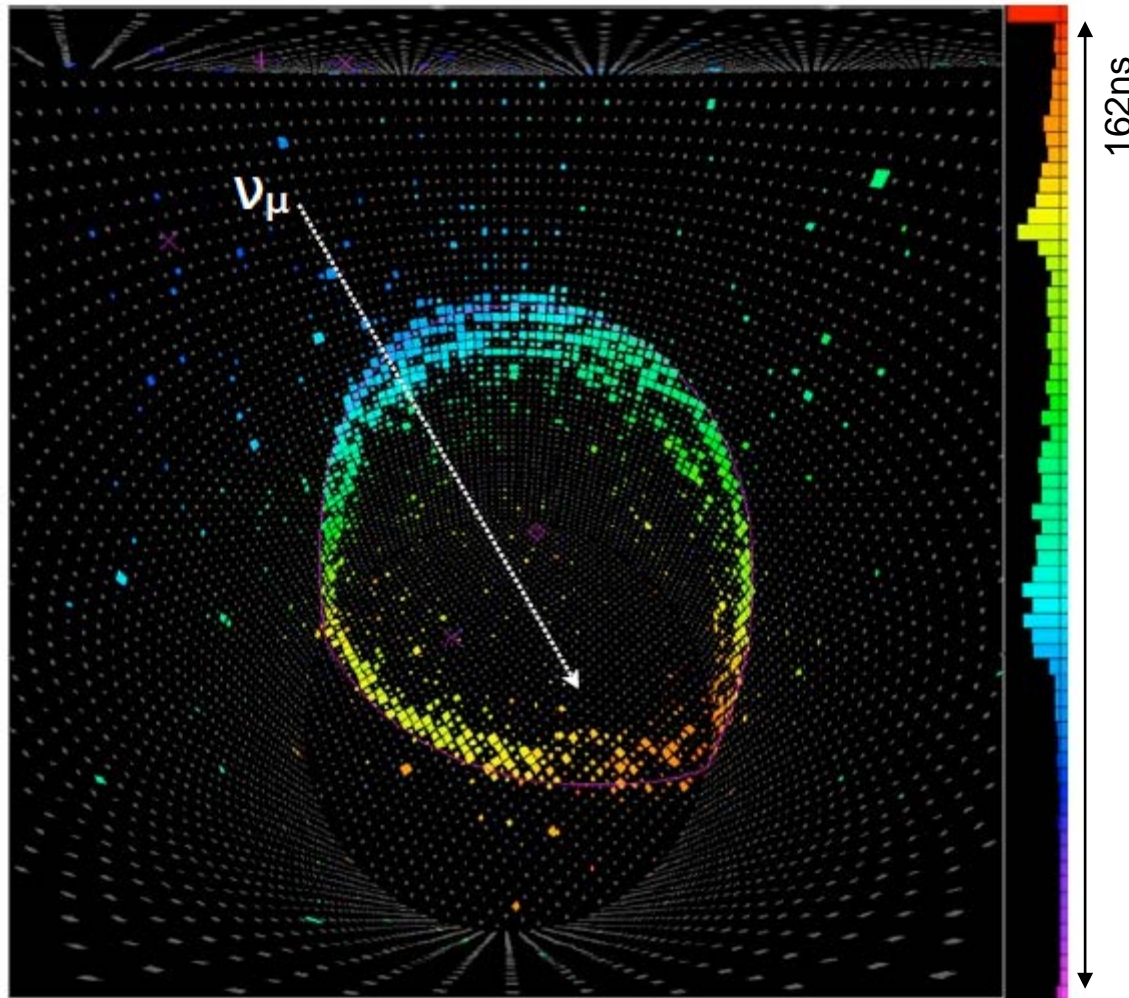
Timing error dominates

Neutrino detection



Direction Measurement

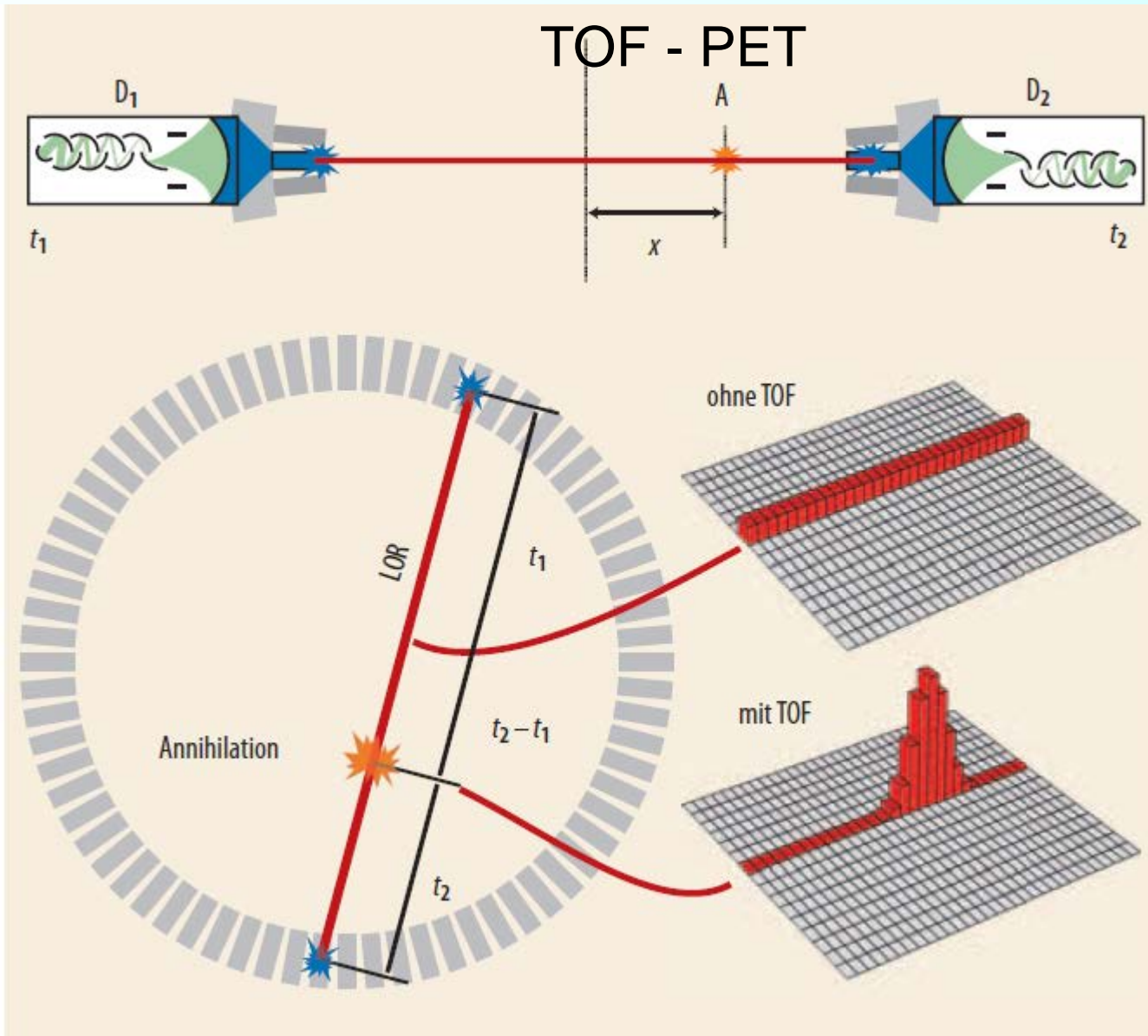
Super – Kamiokande Event Display



muon event (603 MeV)

observation of clean Cherenkov ring with sharp edges
flight direction from timing measurements
blue: early, red: late
energy from amount of light observed in PMs

Timing application for photon detection



C.Degenhard, A.Thon,
Physik Journal 6(2007)23

Spatial resolution:

$$x = \frac{1}{2}c(t_1 - t_2)$$

$$\sigma_x = \frac{1}{2}c \sigma_t$$

1 ns \leftrightarrow 15 cm
 100 ps \leftrightarrow 1.5 cm
 10 ps \leftrightarrow 1.5 mm

Noise Equivalent
 Countrate (NEC)

$$\frac{NEC_{TOF}}{NEC_{noTOF}} \approx \frac{D}{1.6 \cdot \sigma_x}$$

with object size D

Timing techniques and counters

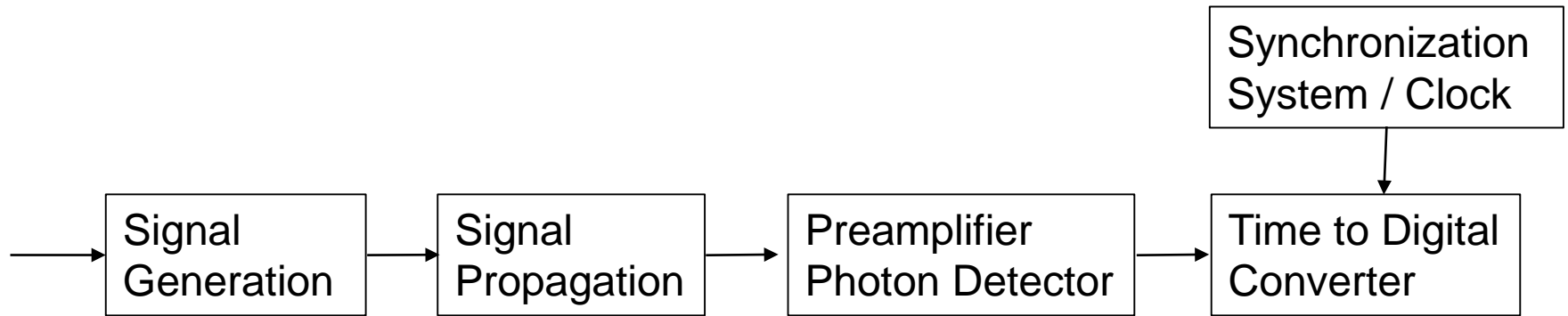
Generalities

Scintillators with PMT (SiPM) readout

Gas counters (MRPC)

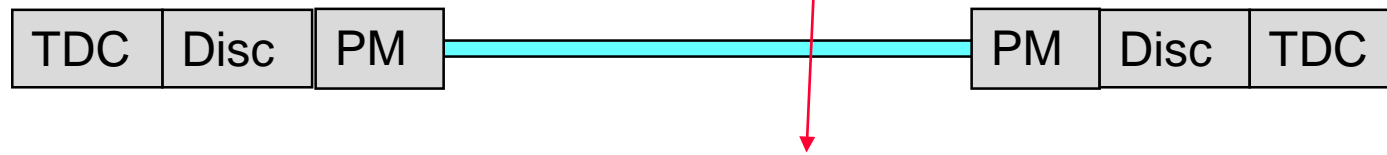
Diamonds

Measurement of Arrival Time



$$\sigma_t^2 = \sigma_{\text{generation}}^2 \oplus \sigma_{\text{transport}}^2 \oplus \sigma_{\text{conversion}}^2 \oplus \sigma_{\text{digitization}}^2$$

Example: plastic slat counter



- 1) Ionization by Bethe-Bloch, scintillation process with decay time $\tau \sim 2$ ns
- 2) Photon propagation, refractive index $n = 1.58$
- 3) Light conversion in photomultiplier with transient time spread
- 4) Discrimination for varying pulse heights (walk or slewing correction needed)
- 5) Digitization with clock synchronization

Note:

Timing resolution in single ended readout is limited by plastic size: $\sigma_t = L \cdot n / (c\sqrt{12})$

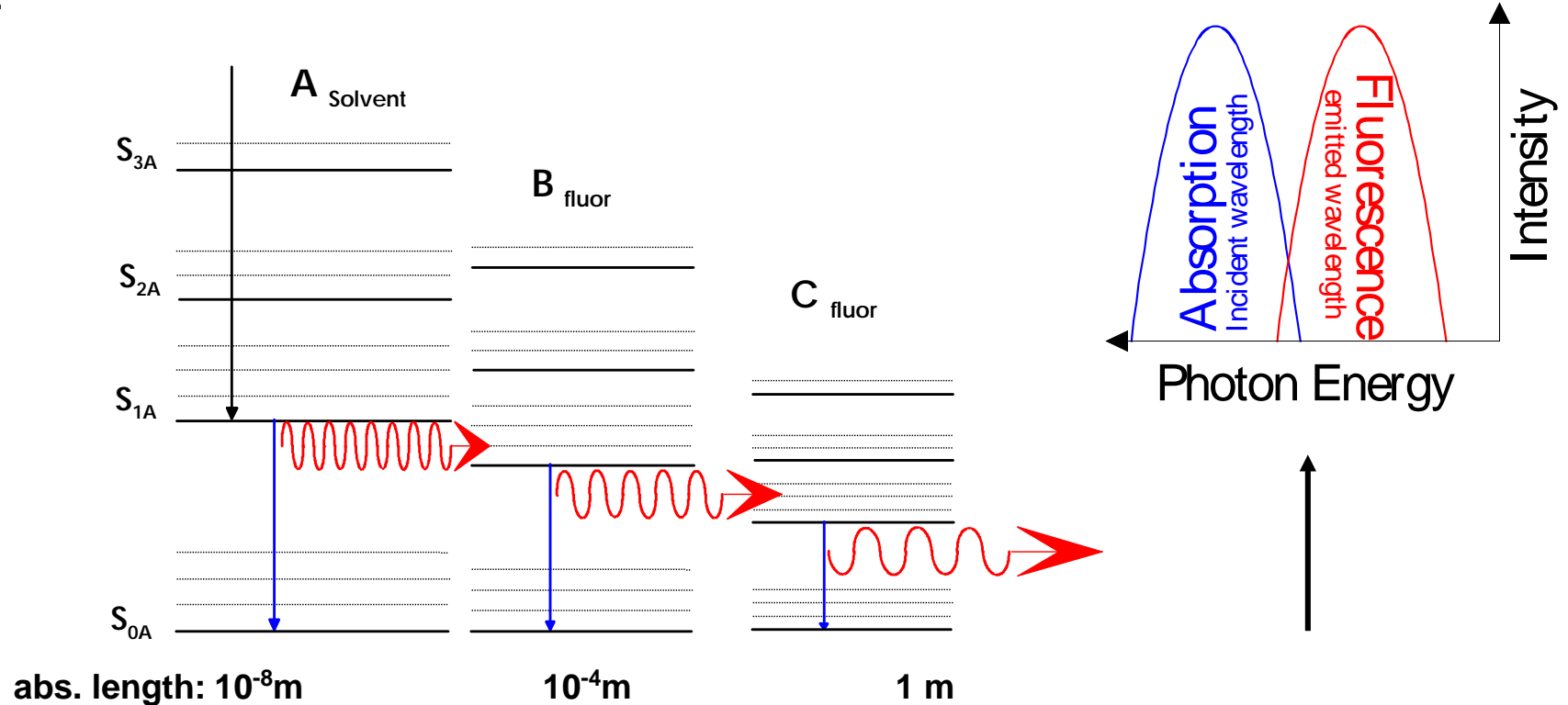
Double sided readout:

$$t = \frac{1}{2} (t_1 + t_2) - L \cdot n / c$$

$$\sigma_t = \frac{1}{\sqrt{2}} \sigma_{t_i}$$

Signal Generation in Plastic Scintillators

Organic scintillators (plastic, liquid) use a solvent
+ large concentration of primary fluor
+ smaller concentration of secondary fluor
+



Fast energy transfer via non-radiative dipole-dipole interactions (Förster transfer).

→ shift emission to longer wavelengths

→ longer absorption length and better matching to photocathode efficiency

Properties of Plastic Scintillators

Scintillator material	Density [g/cm ³]	Refractive Index	Wavelength [nm] for max. emission	Decay time constant [ns]	Photons/MeV
NE102*	1.03	1.58	425	2.5	$2.5 \cdot 10^4$
NE104*	1.03	1.58	405	1.8	$2.4 \cdot 10^4$
NE110*	1.03	1.58	437	3.3	$2.4 \cdot 10^4$
NE111*	1.03	1.58	370	1.7	$2.3 \cdot 10^4$
BC400**	1.03	1.58	423	2.4	$2.5 \cdot 10^2$
BC428**	1.03	1.58	480	12.5	$2.2 \cdot 10^4$
BC443**	1.05	1.58	425	2.2	$2.4 \cdot 10^4$

* Nuclear Enterprises, U.K.

** Bicron Corporation, USA

Typical numbers:

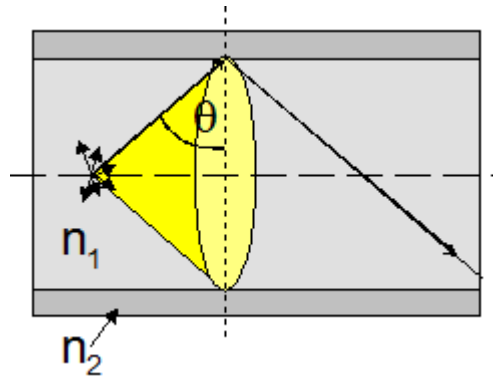
Energy deposition of MIP in 1 cm plastic (Bethe – Bloch)

$$\Delta E \sim 1.7 \text{ MeV}$$

$$\Rightarrow \sim 50.000 \text{ photons}$$

However, only directly propagating ones contain relevant timing information!

Light propagation in plastic slat / fibre



Total internal reflection

$$\theta \geq \arcsin \frac{n_2}{n_1} = \arcsin \frac{1}{1.58} = 39.3^\circ$$

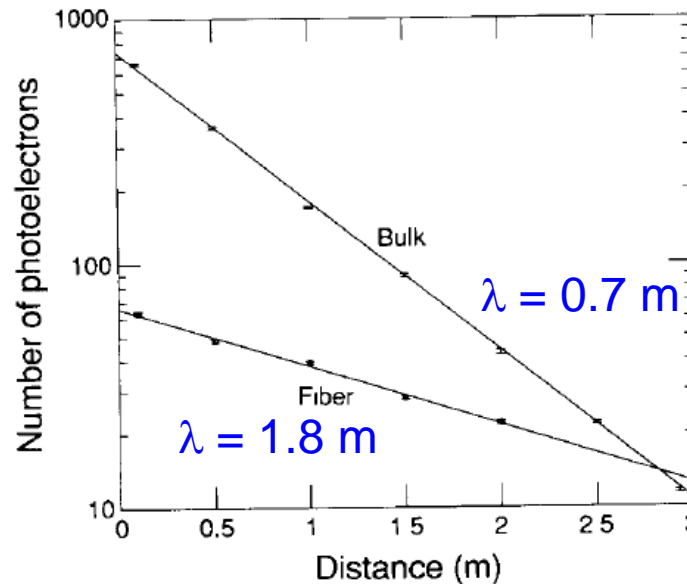
$$\frac{\Delta\Omega}{4\pi} = 18\% \quad \text{best case, when surface is perfect}$$

Light attenuation (absorption):

$$N_{ph} = N_0 e^{-\frac{d}{\lambda}}$$

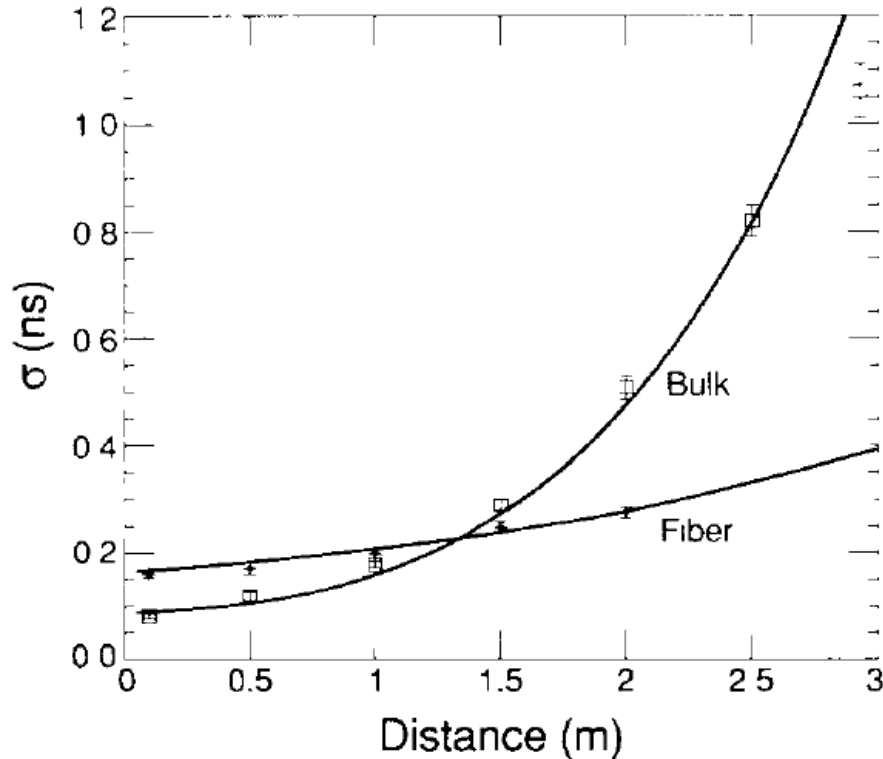
Example for $3 \times 2 \text{ cm}^2$

(bulk counter wrapped with Teflon tape to optimized light yield)



M. Kuhlen et al., NIM A301(1991)223

Impact on light propagation on timing

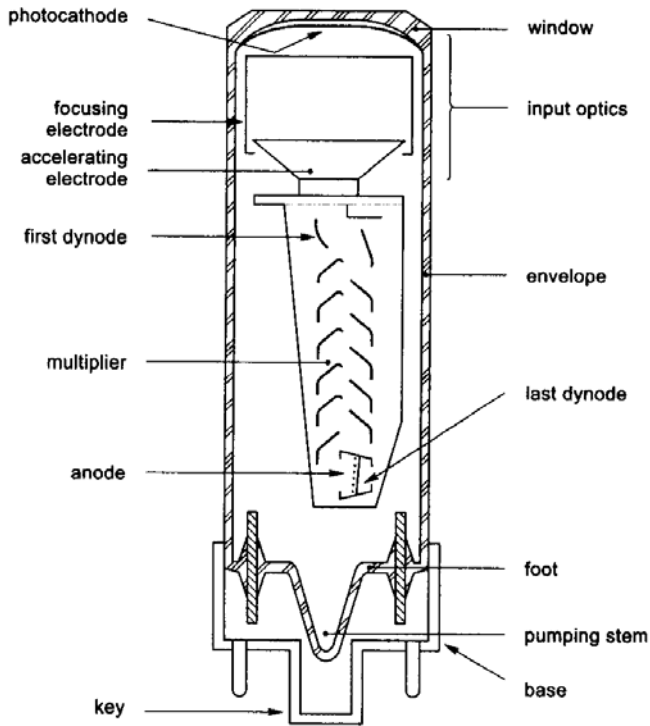


M. Kuhlén et al., NIM A301(1991)223

Timing information is carried by the early photons.
→ design systems with well defined propagation path length.

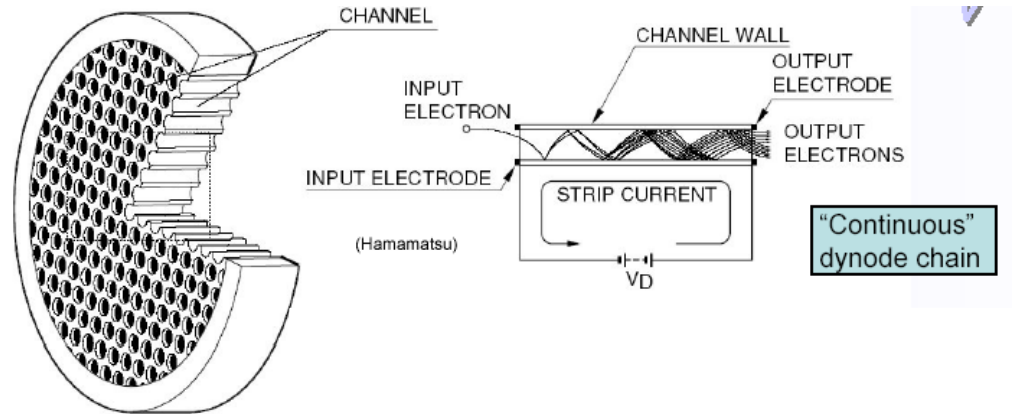
Photosensors

PMT



key feature for timing
 path length variation from
 photoelectrode to first dynode
 → transient time spread

Micro channel plate (MCP)



Hybrid photo diodes (HPD)

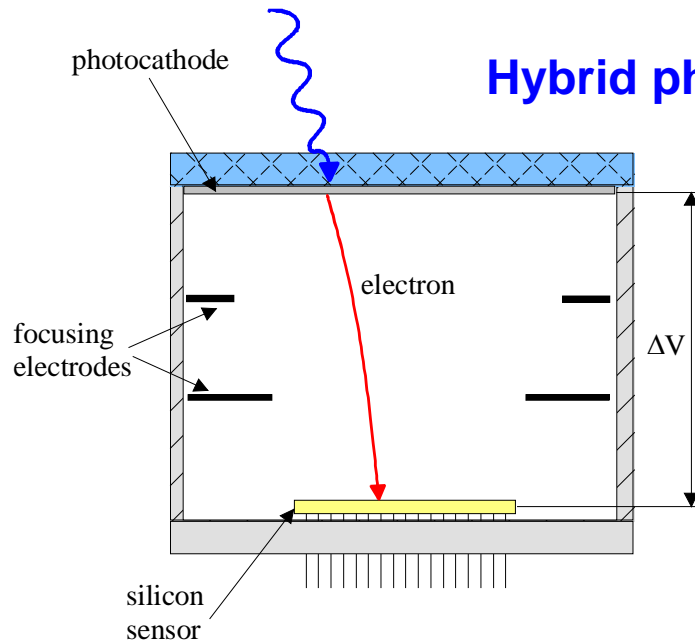


photo cathode + p.e.
 acceleration + silicon
 det. (pixel, strip, pads)

ΔV 10-20 kV

Photon detection

Table 33.2: Representative characteristics of some photodetectors commonly used in particle physics. The time resolution of the devices listed here vary in the 10–2000 ps range.

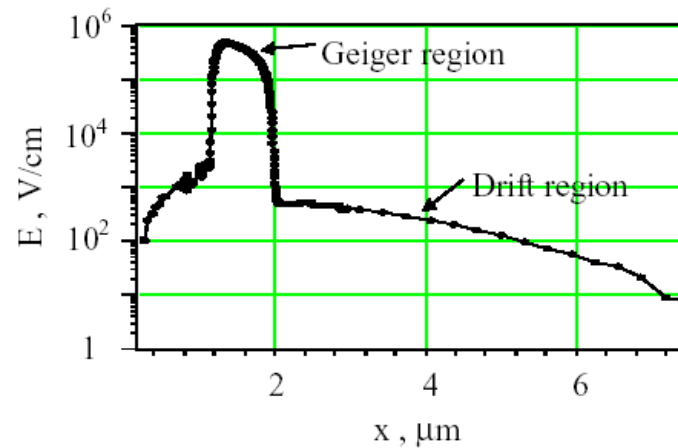
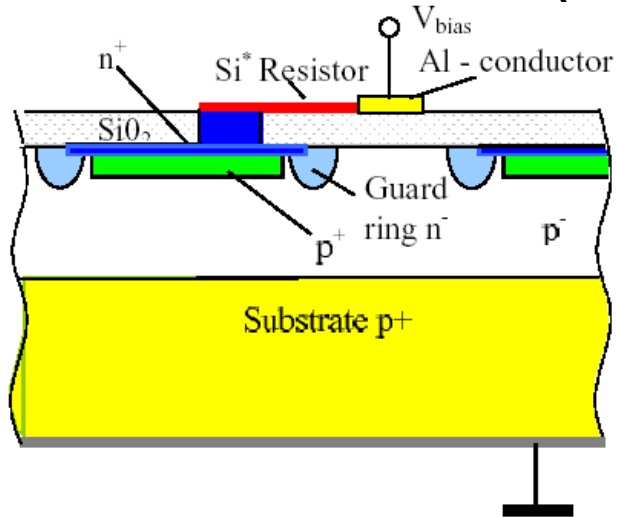
Type	λ (nm)	$\epsilon_Q \epsilon_C$	Gain	Risetime (ns)	Area (mm ²)	1-p.e noise (Hz)	HV (V)	Price (USD)
PMT*	115–1700	0.15–0.25	10^3 – 10^7	0.7–10	10^2 – 10^5	10 – 10^4	500–3000	100–5000
MCP*	100–650	0.01–0.10	10^3 – 10^7	0.15–0.3	10^2 – 10^4	0.1–200	500–3500	10–6000
HPD*	115–850	0.1–0.3	10^3 – 10^4	7	10^2 – 10^5	10 – 10^3	$\sim 2 \times 10^4$	~ 600
GPM*	115–500	0.15–0.3	10^3 – 10^6	$O(0.1)$	$O(10)$	10 – 10^3	300–2000	$O(10)$
APD	300–1700	~ 0.7	10 – 10^8	$O(1)$	10 – 10^3	1 – 10^3	400–1400	$O(100)$
PPD	320–900	0.15–0.3	10^5 – 10^6	~ 1	1–10	$O(10^6)$	30–60	$O(100)$
VLPC	500–600	~ 0.9	$\sim 5 \times 10^4$	~ 10	1	$O(10^4)$	~ 7	~ 1

*These devices often come in multi-anode configurations. In such cases, area, noise, and price are to be considered on a “per readout-channel” basis.

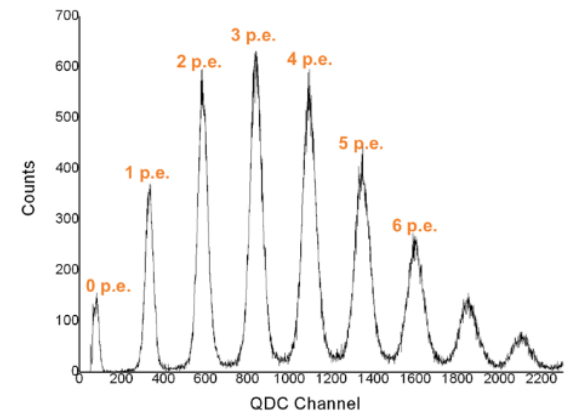
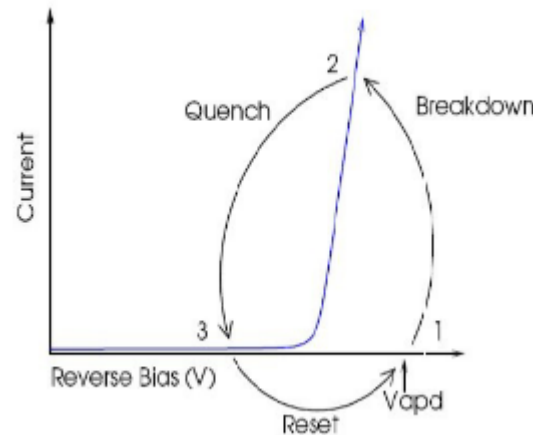
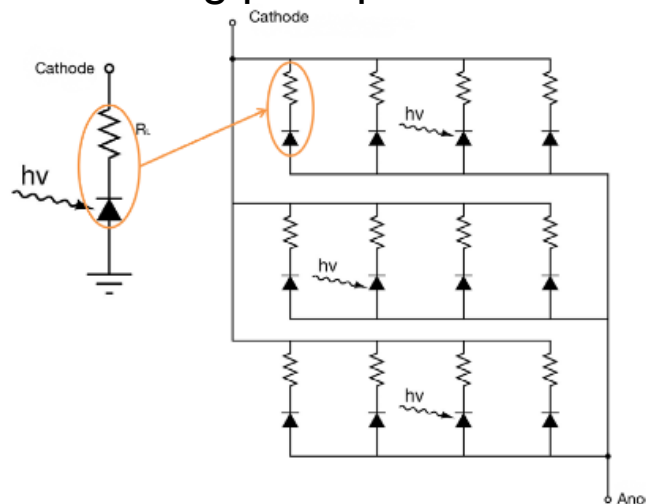
Commercially available timing sensors (PMT, MCP) with suitable rise times (< 1 ns) are very expensive: ~ 1000 €/ channel
except for PPD (SiPM)

Solid State Photosensors: SiPM

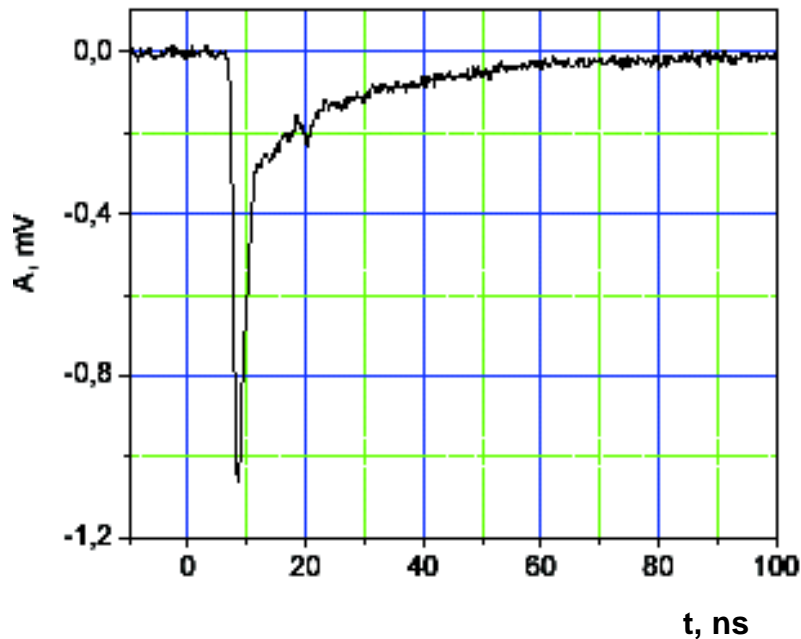
Silicon – Photomultiplier (APD in Geiger mode)



Working principle:



Timing Characteristics of SiPM



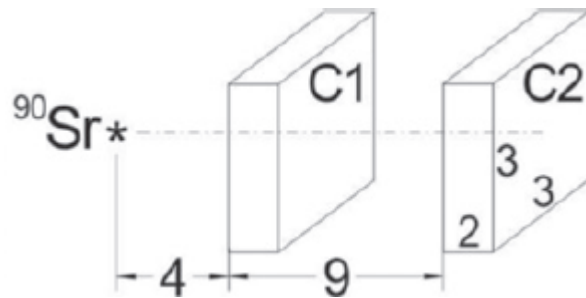
- Fast Geiger discharge development
< 500 ps
- Discharge is quenched by current limiting with polysilicon resistor in each pixel
 $I < 10 \mu\text{A}$
- Pixel recovery time
 $\sim C_{\text{pixel}} R_{\text{pixel}} = 100 - 500 \text{ ns}$

Low noise, high bandwidth electronics required

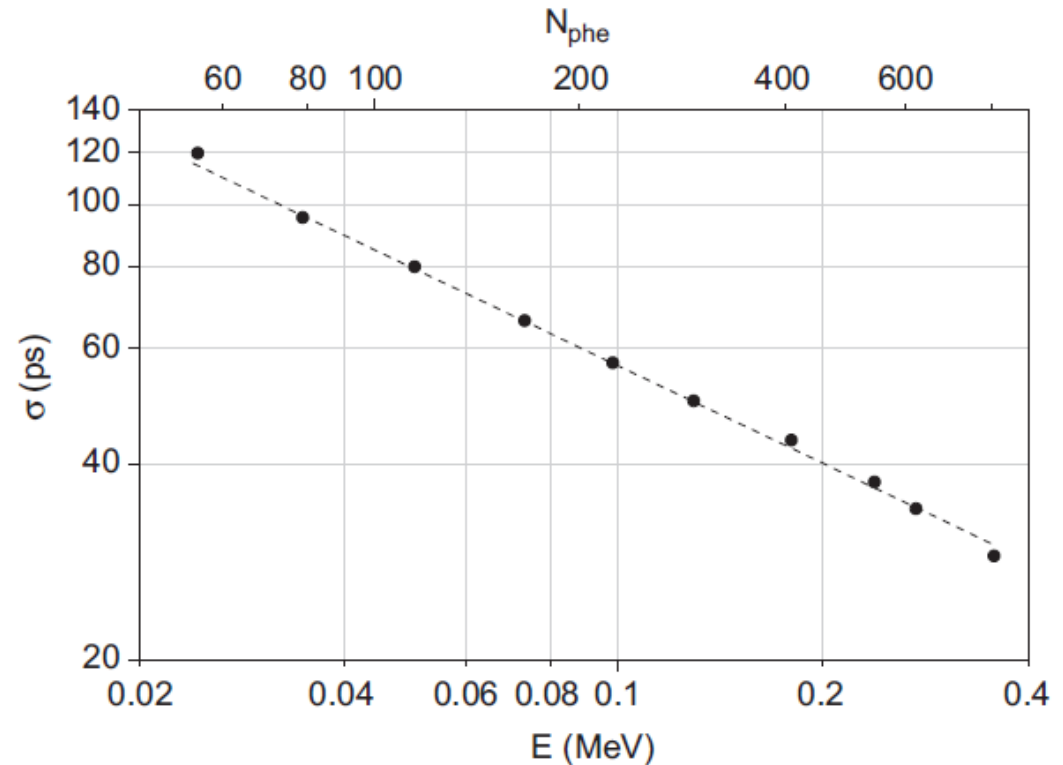
$$\sigma_t = \frac{\sigma_{\text{noise}}}{\left. \frac{dS}{dt} \right|_{S_{\text{threshold}}}} \approx \frac{t_{\text{rise}}}{S/N}$$

Plastic & SiPM

A. Stoykov et al., NIM A 695 (2012) 202



Scintillators coupled to
Hamamatsu MPPC
S10362-33-050
(3 x 3 mm², 3600 pixel)



Achieved time resolution: as good as for PMT!

$$\sigma_t = 18 \text{ ps} / \sqrt{E / 1 \text{ MeV}}$$

Electron TOF counter with Plastic & SiPM

P.W. Cattaneo et al. (MEGII), arXiv:1402.1404v2 [physics.ins-det]

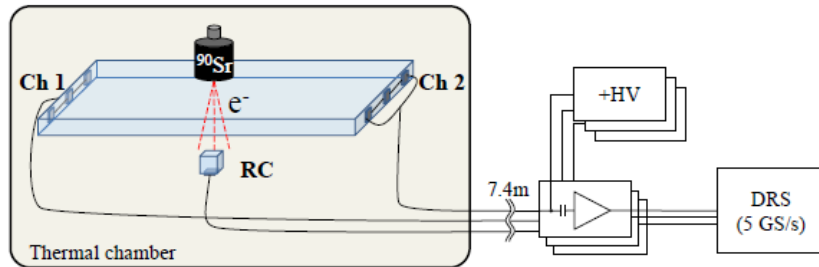
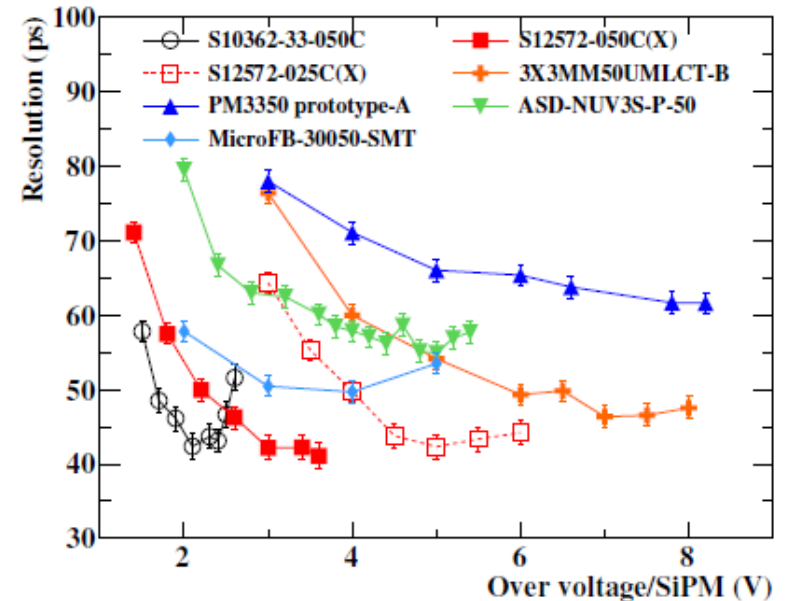
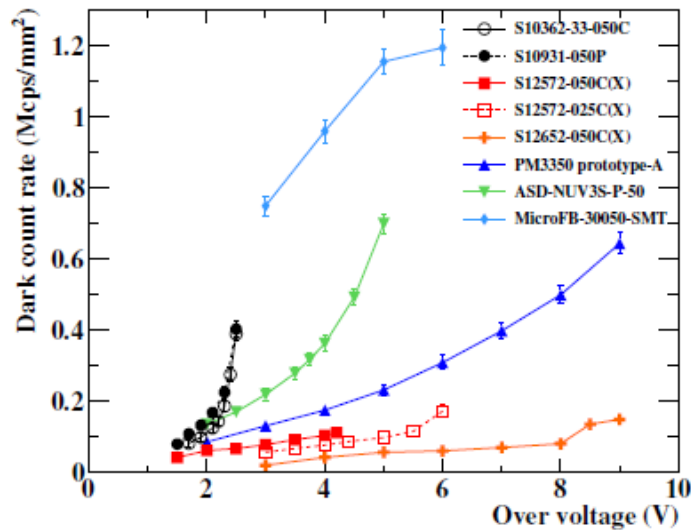
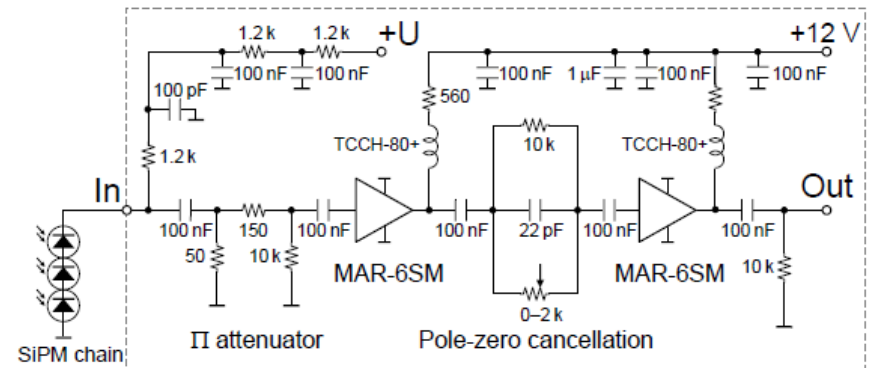


Fig. 1. Test setup for measurements of the counter time resolution. RC denotes the reference counter. See the text for details.



Neutron TOF counter with Plastic & SiPM

T.P. Reinhardt et al. (R3B), NIM A816 (2016) 16

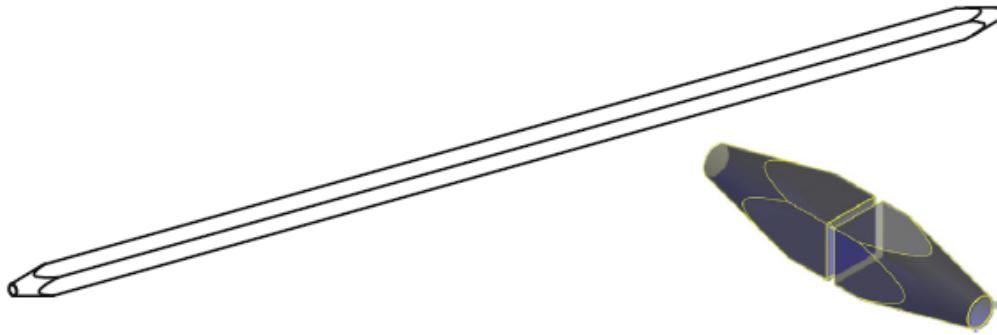
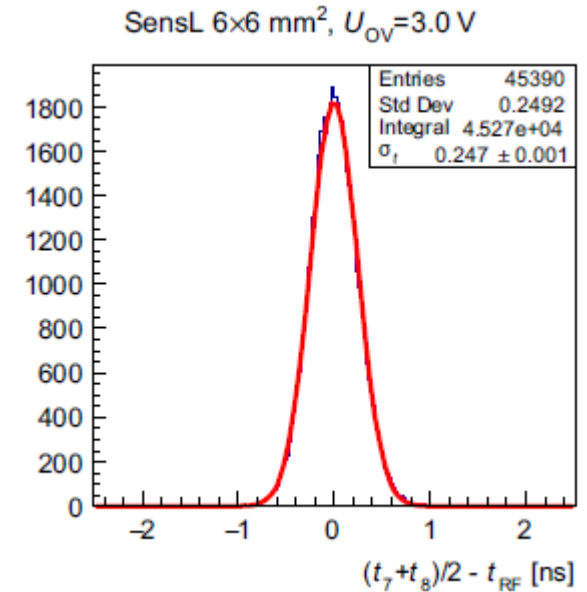


Fig. 1. NeuLAND bar. The left side shows the entire, 270 cm long NeuLAND bar. The right side shows the two tapered sides converting from $5 \times 5 \text{ cm}^2$ square shape to $d=2.5 \text{ cm}$ circular shape.



Test beam results with
30 MeV e^- @ ELBE

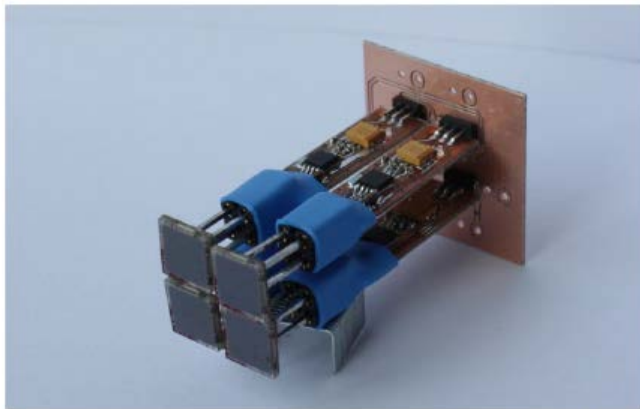


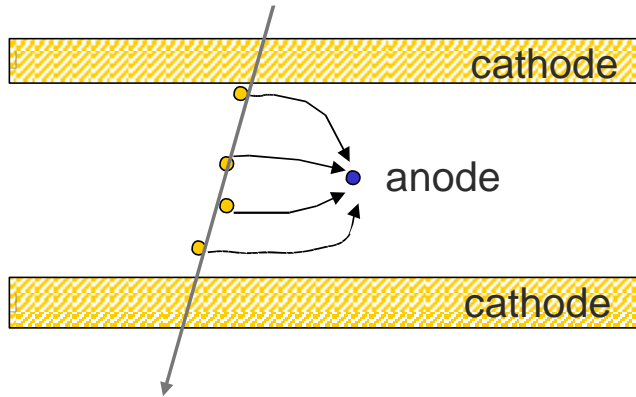
Fig. 2. Photograph of the preamplifier board, complete with four $6 \times 6 \text{ mm}^2$ SiPMs. When in use, the SiPMs are separated from the board by a neoprene layer that is penetrated by the pin connectors of the SiPMs.

Performance better than with PMT
(although not all the area was covered with sensors)

Efficiency: $99 \pm 1 \%$

Timing resolution: $\sigma_t = 136 \pm 2 \text{ ps}$

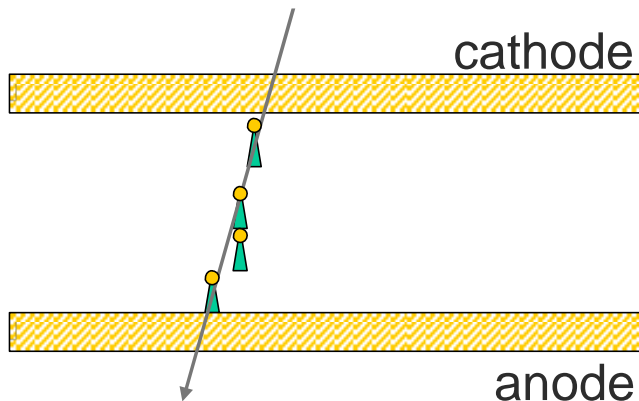
Timing with Gas Counters



Problem:

“slow” drift of electrons from primary ionization to amplification region

$$v_{\text{drift}} \sim 10 \mu\text{m/ns}$$

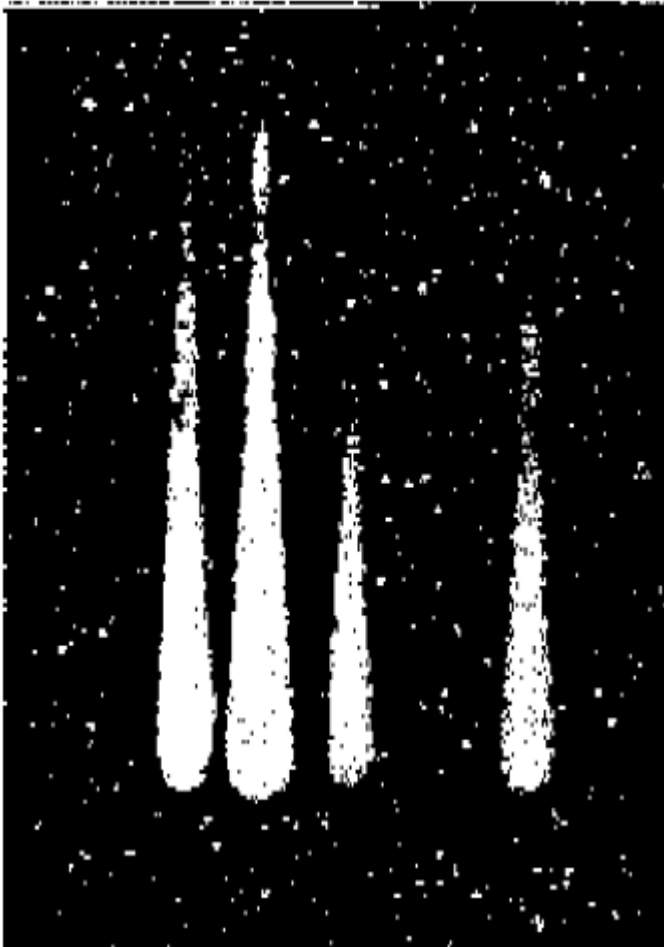


Concept:

detect avalanches directly,
large E-field in whole detector volume

Electron multiplication

Cloud chamber picture of electron avalanches in parallel plate counter



W. Legler, Z. Naturforschung 16a, 253 (1961)

$$\frac{d\bar{n}}{dx} = \underbrace{(\alpha - \eta)}_{\alpha_{eff}} \bar{n}$$

\bar{n} - average electron number

\bar{p} - average positive ion number

α - Townsend coefficient

$$\frac{d\bar{p}}{dx} = \alpha \bar{n}$$

η - attachment coefficient

(electron can get attached to an atom forming a negative ion)

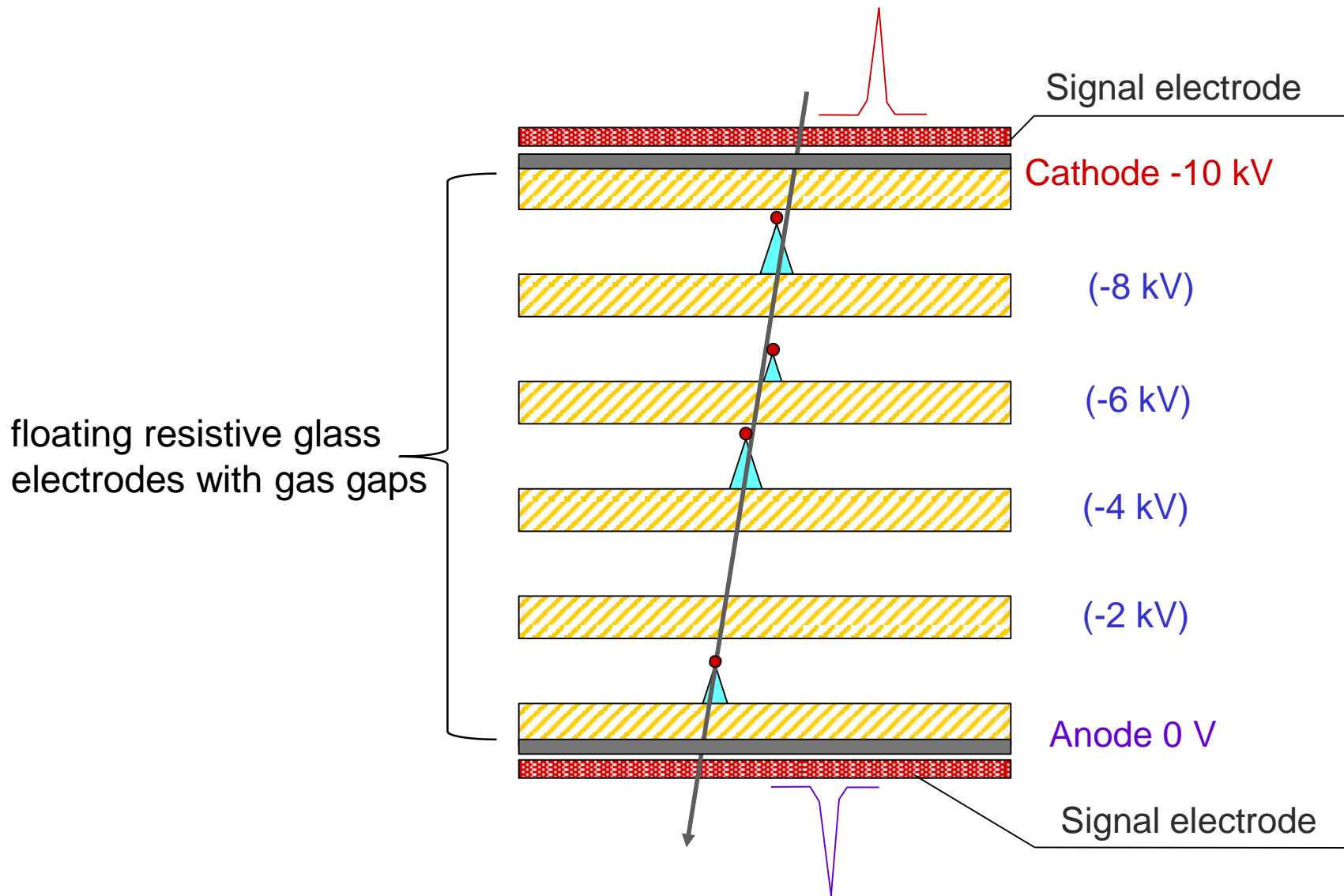
$$\bar{n}(0) = 1,$$

$$\bar{n}(x) = e^{(\alpha - \eta)x}$$

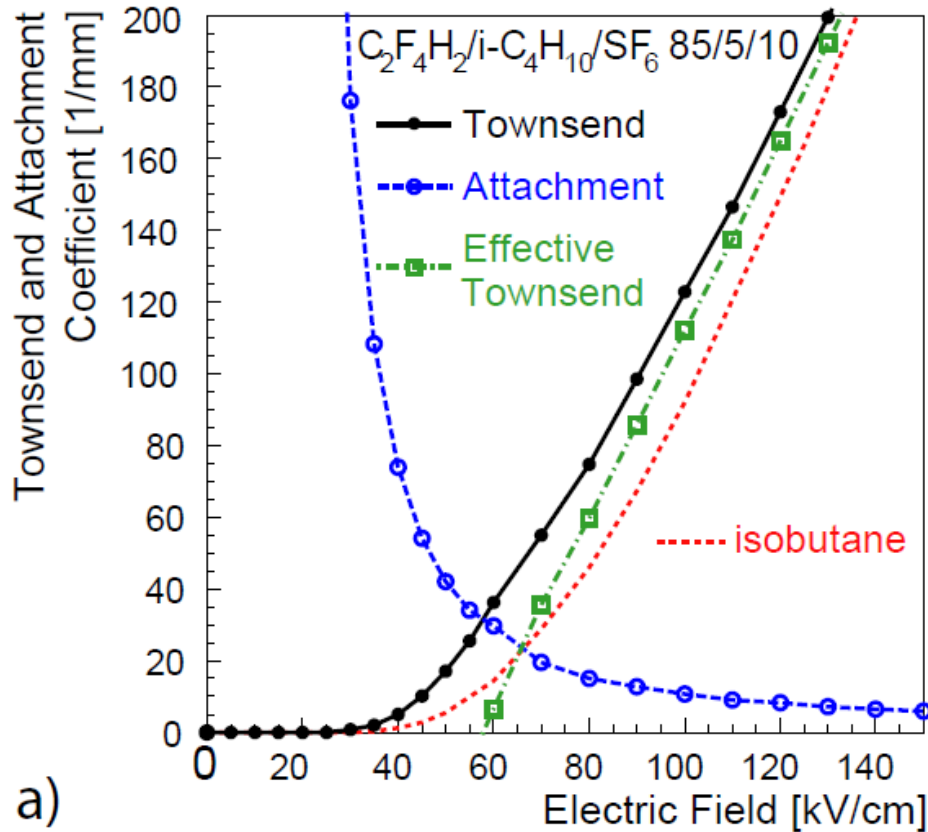
$$\bar{p}(0) = 0$$

$$\bar{p}(x) = \frac{\alpha}{\alpha - \eta} \left(e^{(\alpha - \eta)x} - 1 \right)$$

Multi-gap Resistive Plate Chamber



Avalanche growth



W. Riegler, C. Lippmann, R. Veenhof
NIM A500 (2003) 144
IMONTE calculation: S. Biagi (CERN)

Operating point:

$E=100$ kV/cm

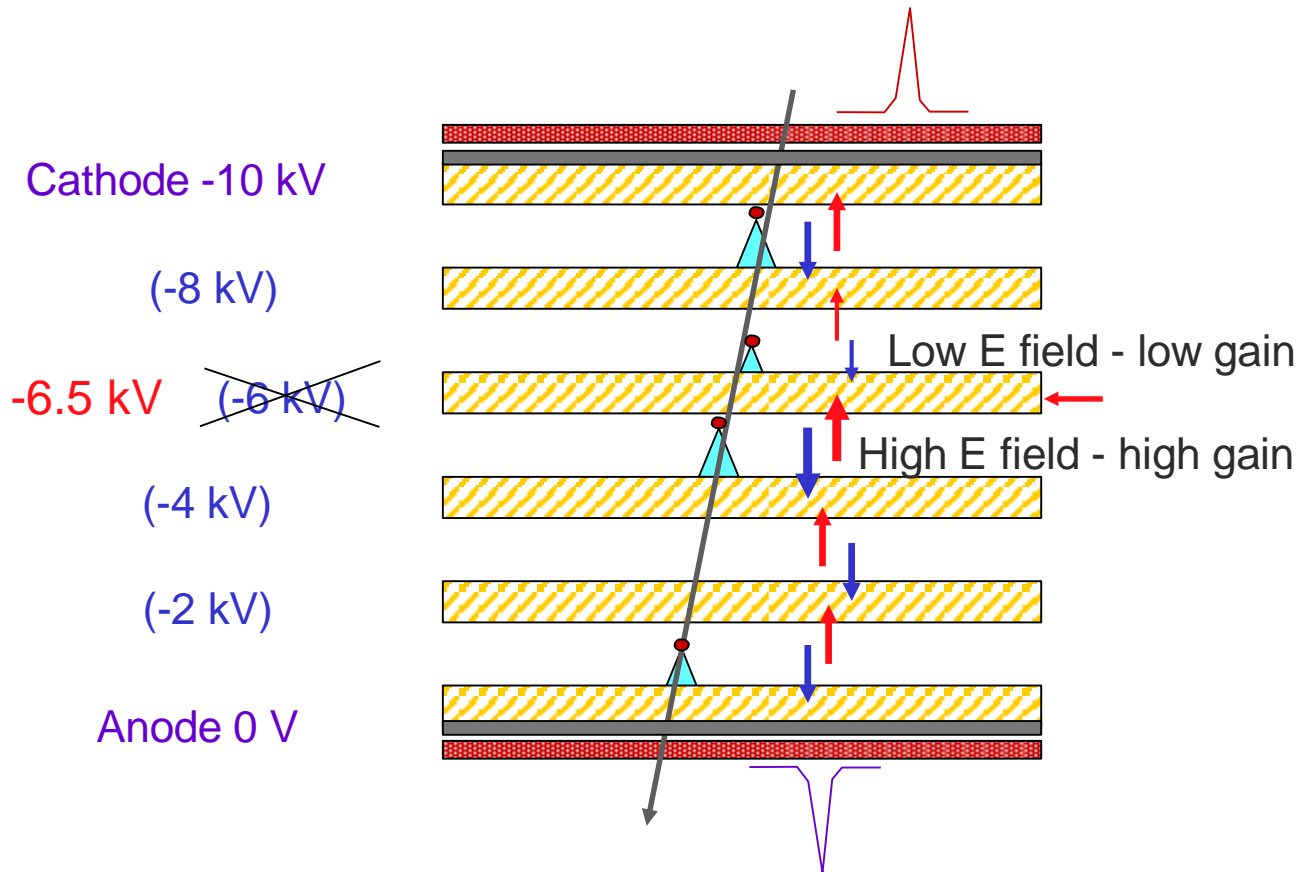
$\alpha_{\text{eff}} = 100$ / mm

Over a distance of 0.2 mm
a single electron would generate
 $5 \cdot 10^8$ electrons ($Q=80$ pC).

However: space charge effects!

Raether limit: multiplication $M < 10^8$, $\alpha x < 20$

Stability of operation



Avalanche gain dependence automatically corrects potentials on the resistive plates – stable situation is "equal gains in all gas gaps"

Signal generation

W. Riegler, NIM A491, 258 (2002)

Mechanism: **Induction**

Ramo's theorem:

Assume perfectly conducting electrodes:

$$I(t) = Q\vec{E}(\vec{x}) \cdot \dot{\vec{x}}(t)$$

$\vec{E}(\vec{x})$ – static electric field

with resistive elements;

$$I(t) = \frac{E_w \cdot v_{\text{drift}}}{V_w} e_0 N(t)$$

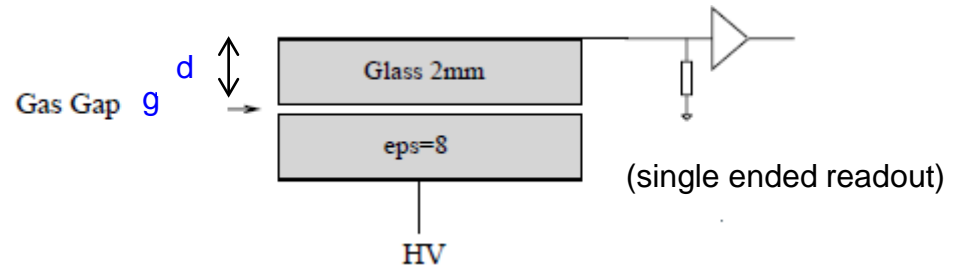
electrons generate the signal

$N(t)$ – number of electrons in avalanche

E_w – weighting field, V_w – weighting potential

$$\frac{E_w}{V_w} = \frac{\epsilon_r}{2d + g\epsilon_r}$$

from $\sum_{i=1}^b E_i d_i =$, with $\epsilon_i E_i = \epsilon_j E_j$ for neighbouring layers



Intrinsic timing resolution

Timing determined by crossing
a discriminator threshold

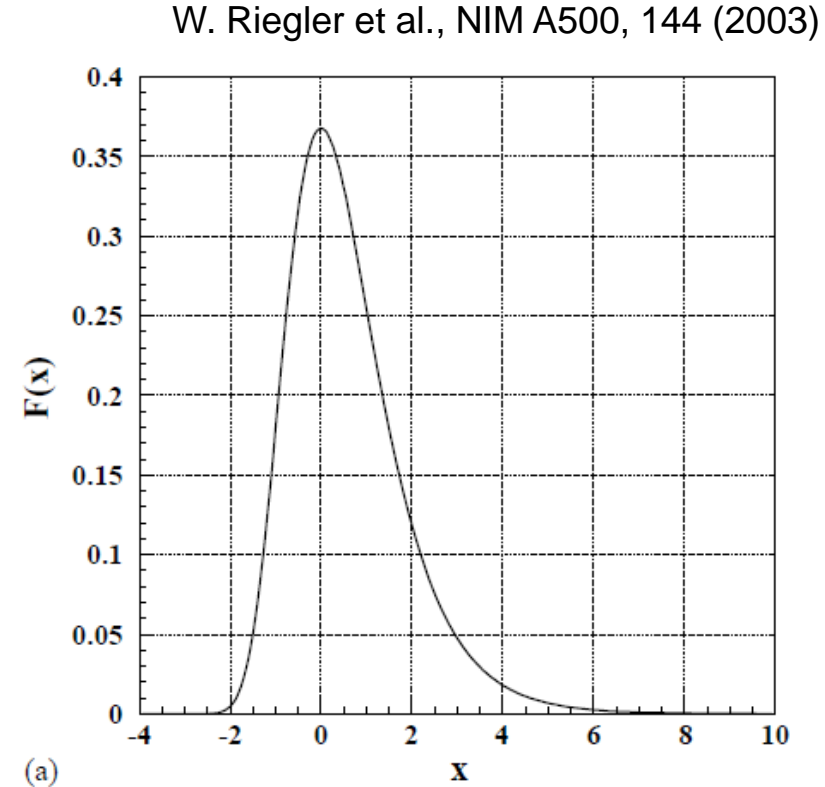
- sufficiently fast amplifier
- low threshold,
- no saturation effects

$$i(t) = Ae^{(\alpha-\eta)vt} = A_{\text{thr}}$$

Probability to cross threshold at time t:

$$P(t) = (\alpha - \eta)vF((\alpha - \eta)vt)$$

$$F(x) = \exp(x - \exp(-x))$$



Time resolution of single gap:

$$\sigma_t = \frac{1.28}{(\alpha - \eta)v}$$

Operating point:

$$E = 100 \text{ kV/cm}$$

$$\alpha_{\text{eff}} = 100 \text{ / mm}$$

$$v = 200 \text{ } \mu\text{m/ns}$$

$$\Rightarrow \sigma_t = 64 \text{ ps}$$

04/04/2016

Efficiency

Induced charge has to pass threshold:

For single primary electron:

$$Q_{ind}(x) = \frac{E_W}{V_W} \frac{e_0}{\alpha - \eta} e^{(\alpha - \mu)(d-x)} - 1$$

⇓

$$\varepsilon = 1 - e^{-\left(1 - \frac{\eta}{\alpha}\right) \frac{d}{\lambda}} \left[1 + \frac{V_W}{E_W} \frac{\alpha - \eta}{e_0} Q_{thr} \right]^{\frac{1}{\alpha \lambda}}$$

(λ is average distance of primary clusters.)

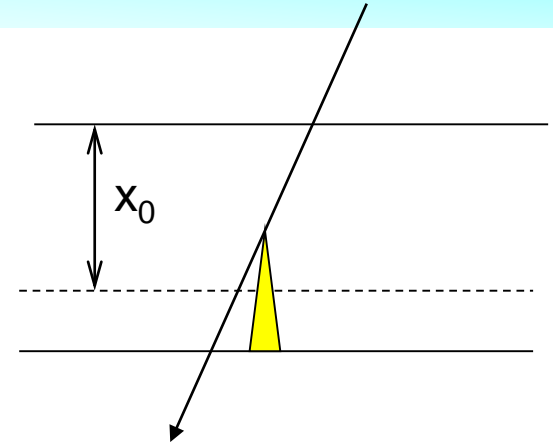
Single gap efficiency at operating point

$$\varepsilon = 80 \%$$

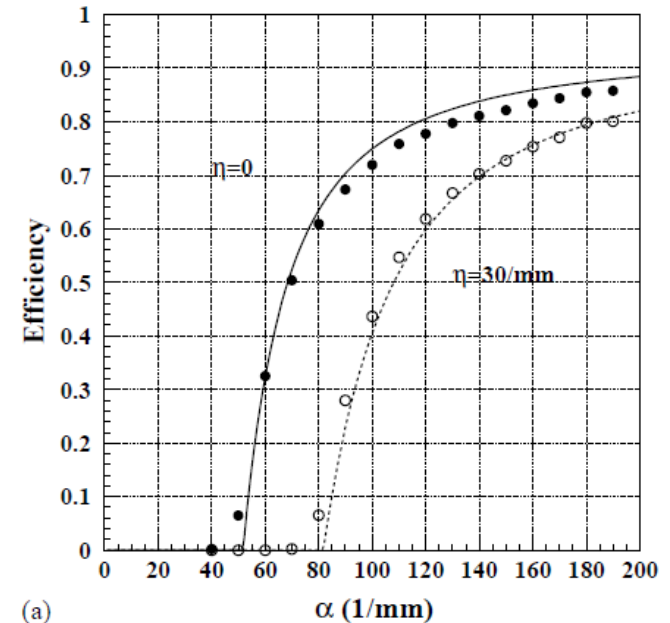
→ multigap configuration needed.

Note: explicit dependence on α and η

-> gas mixture



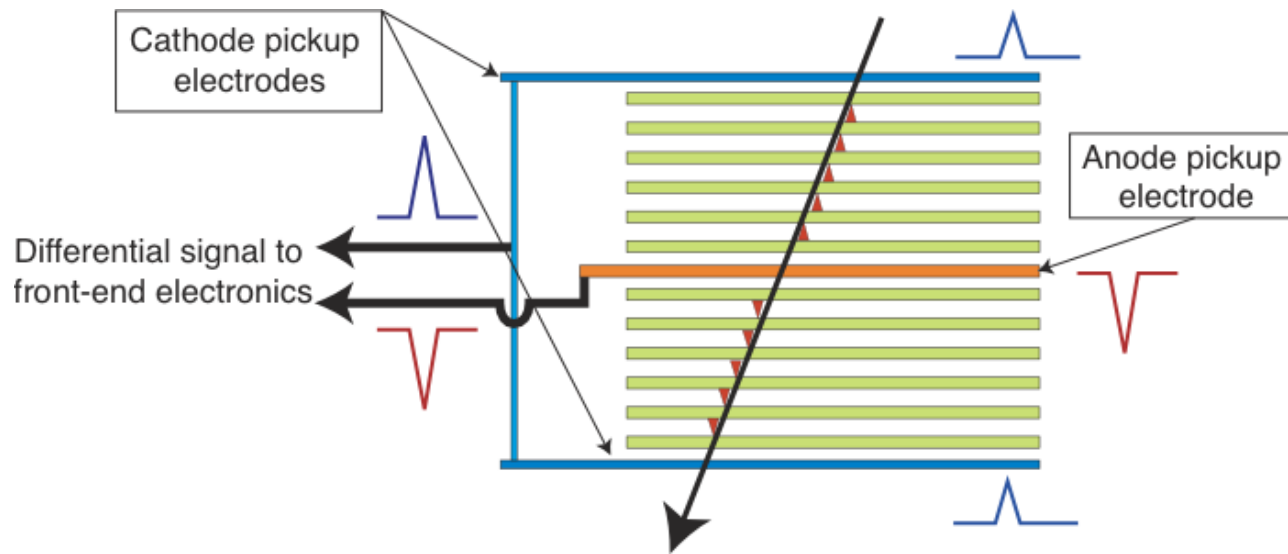
W. Riegler, NIM A **508** (2003) 14



(a)

ALICE – TOF

Features: 10 gas gaps, each of 250 micron width,
built in the form of strips, each with an active area of 120 x 7 cm²,
readout by 96 pads (each 2.5 x 3.5 cm²)

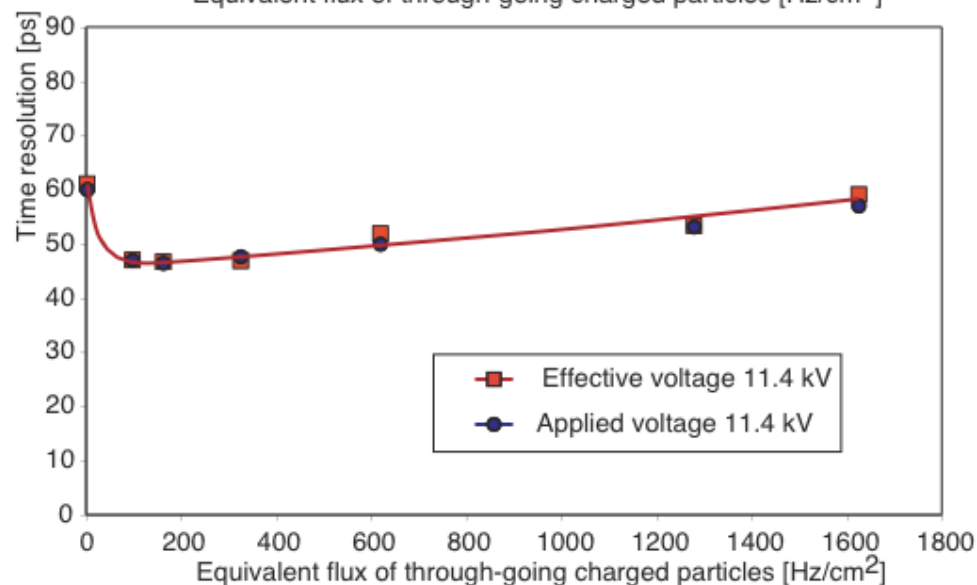
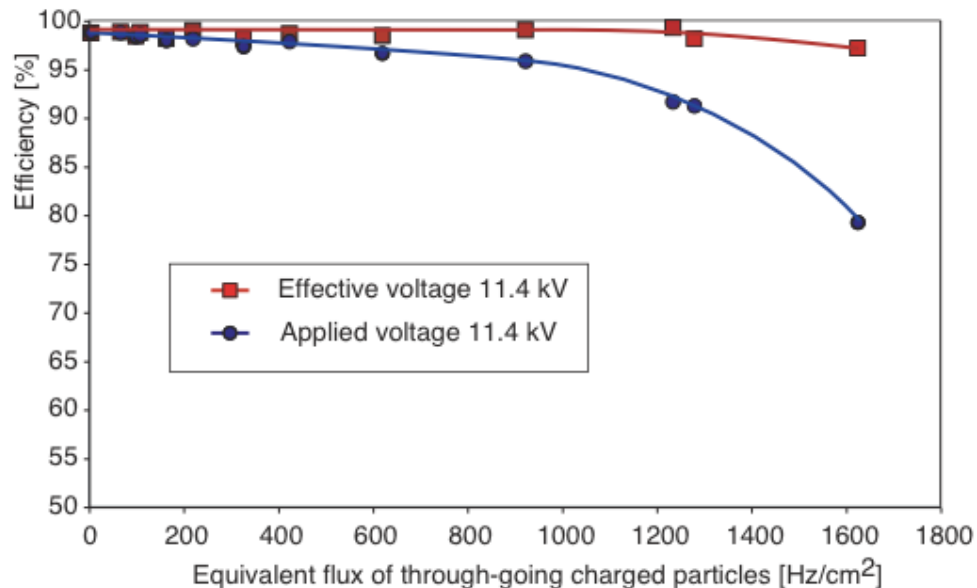


Timing depends on individual gap

Efficiency depends on total gas gap (10x250 μm)

Signal rise time ~ 100 ps, pulse height $\sim 5\text{mV}$ @ 100 Ω -> fast electronics: NINO chip

ALICE – TOF rate capability



Test of 220 micron 10 gap MRPC at GIF CERN

Effective voltage : voltage applied across stack - voltage drop (due to current drawn by MRPC)

Capability in excess of 1 kHz/cm²
Excellent for resistive plate chamber

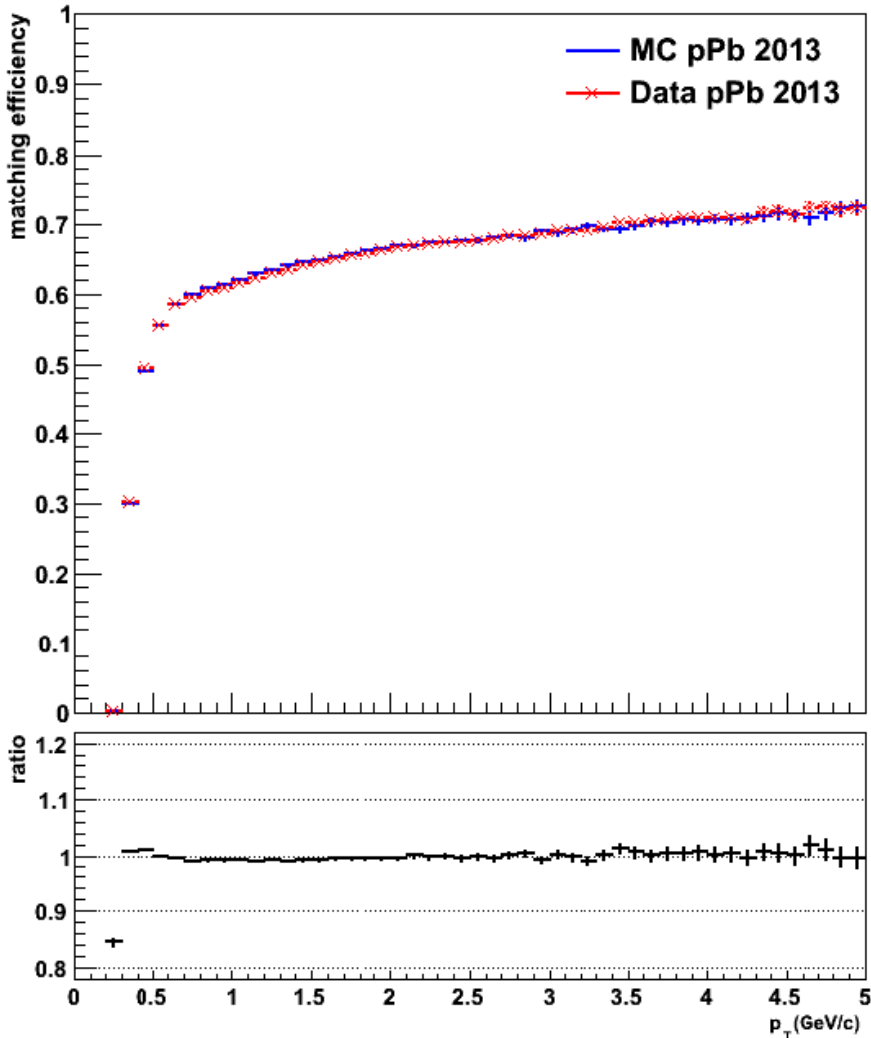
NOTE

glass resistivity $10^{13} \Omega\text{cm}$ in lab
Small average total charge (2 pC)

Nucl. Instr.Meth. A 490 (2002) 58-70

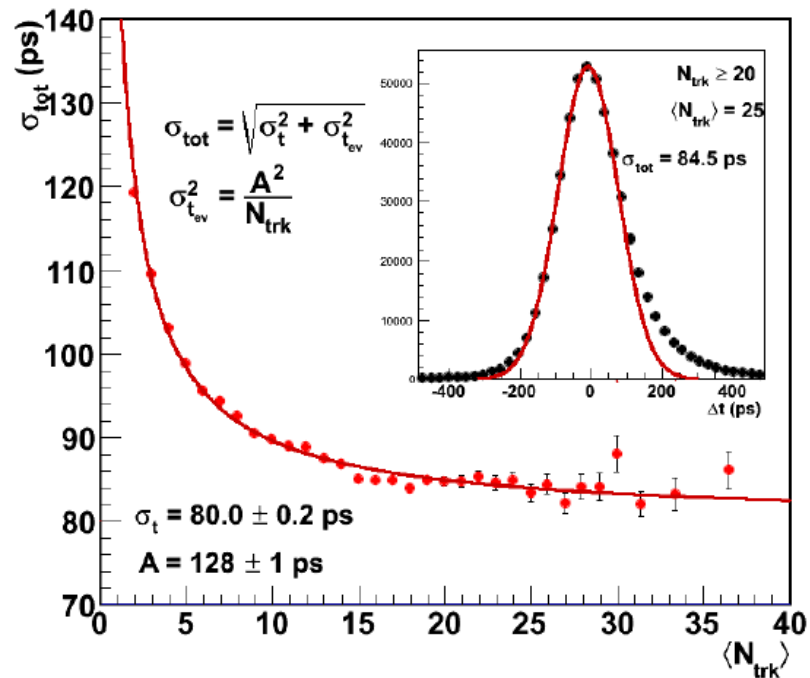
ALICE – TOF in beam performance

Track matching efficiency



Time resolution

from pions with $0.95 < p < 1.05$ GeV/c



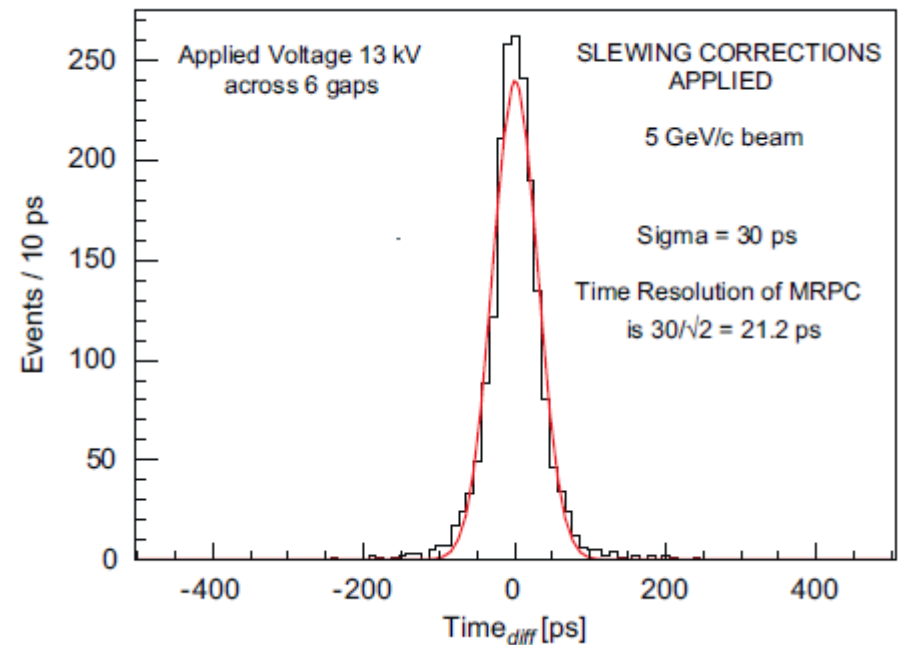
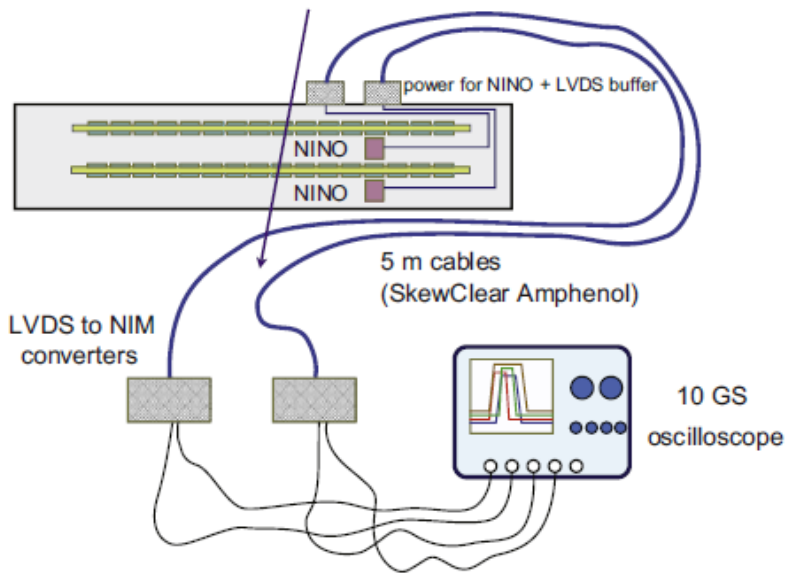
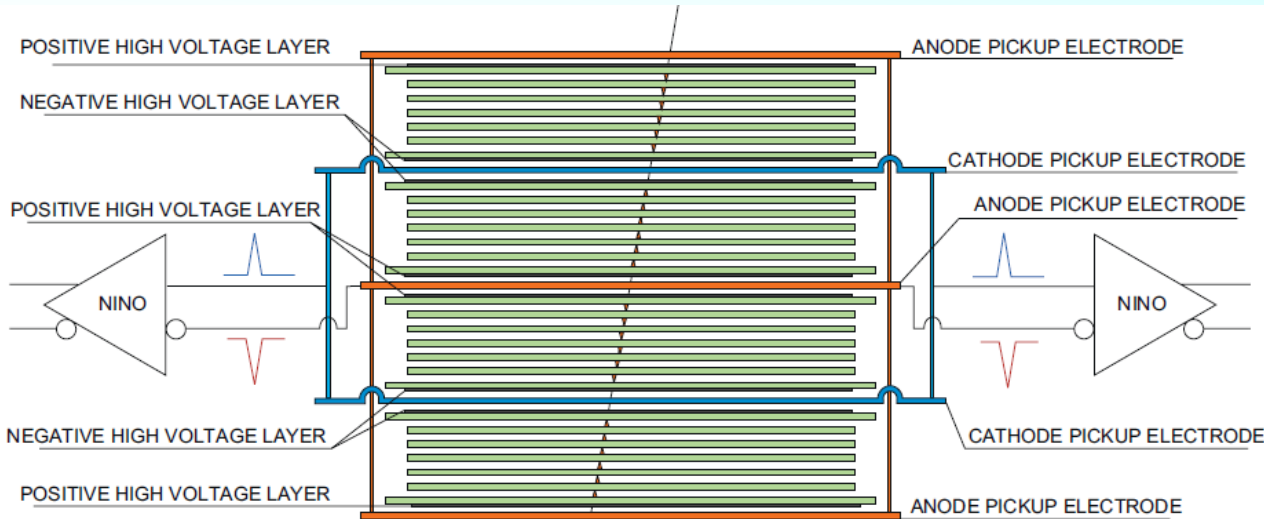
Performance differs from test beam results,
... not fully understood...

20 ps timing device

S. An et al., NIM A594, 39 (2008)

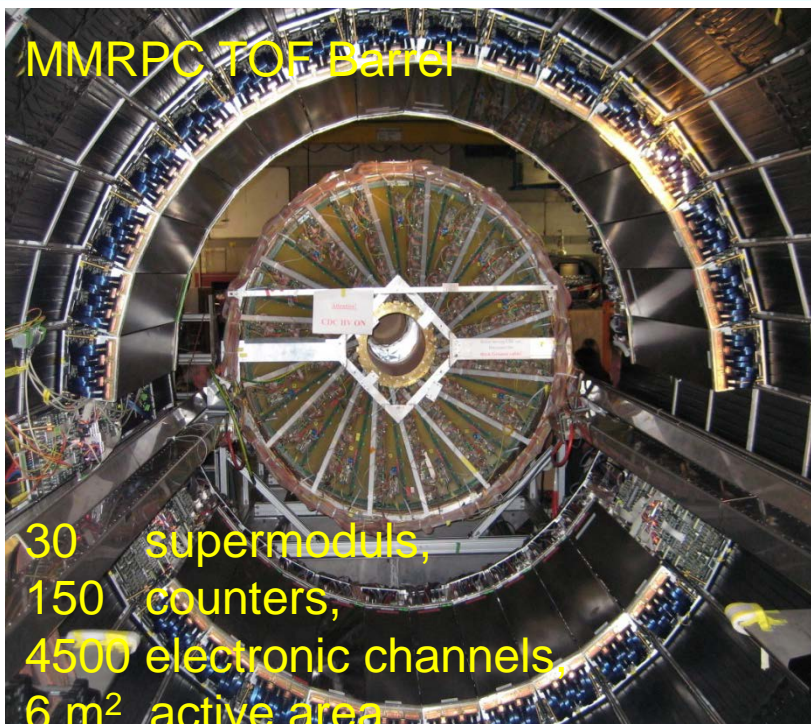
24 gaps of 160 μm

10 ps resolution possible
with 10GHz oscilloscopes
as DAQ system



04/04/2010

FOPI – MMRPC system



M. Kis et al. (FOPI), NIM A 646, 27 (2011)

Multistrip – Multigap – RPC

Developed 2001 – 2005

Construction 2005 – 2007

Operation 2007 - 2011

Features:

8 gaps of 250 μm

length: 90 cm

pitch: 2.54 mm

Impedance: 50 Ω

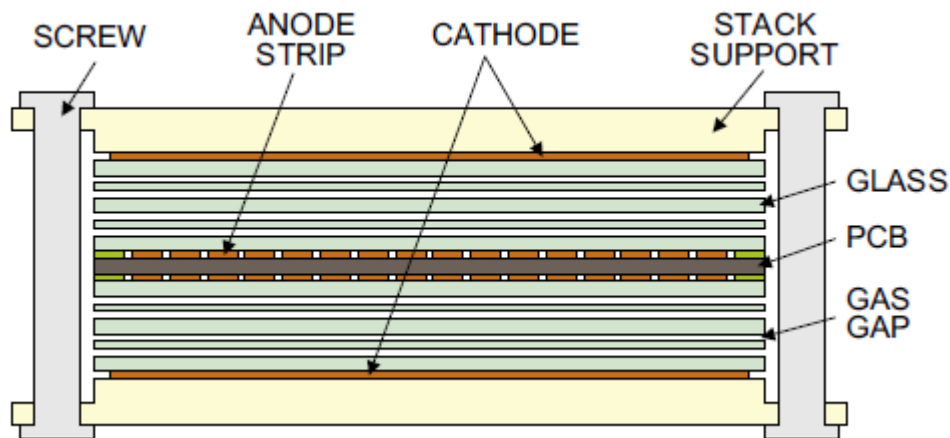
16 readout strips per counter

single ended readout

Signal distributed on several strips

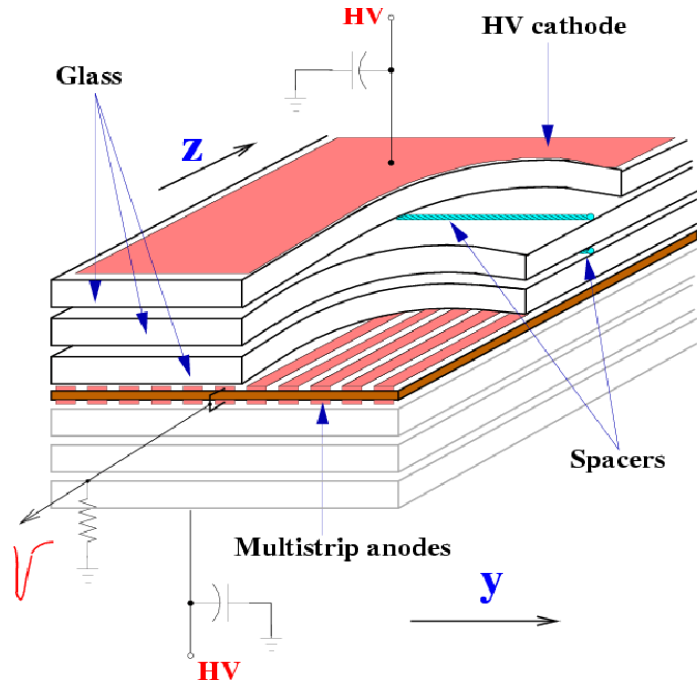
→ high demands on preamplifier

→ PADI chip development



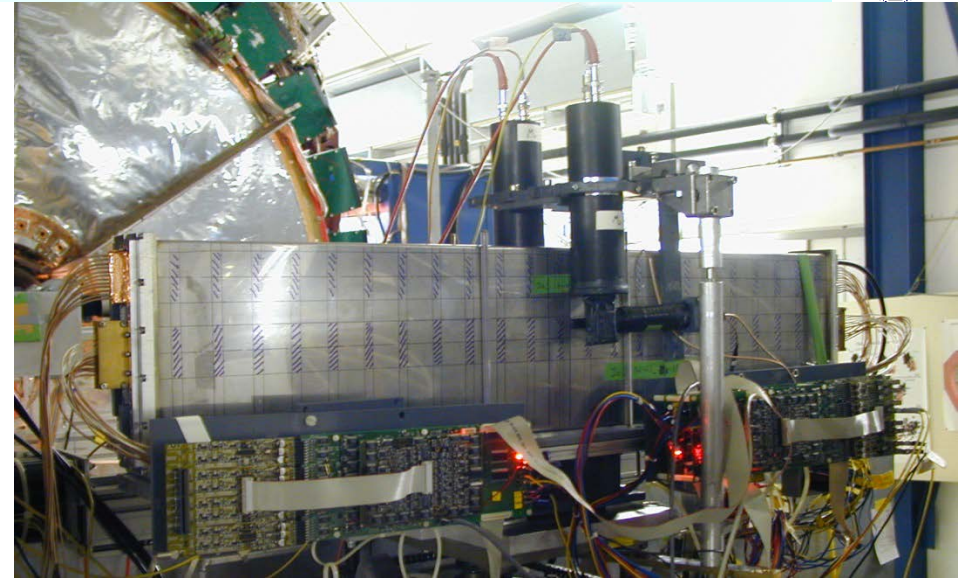
FOPI-Resistive Plate Chambers (RPC)

1. full size prototype, Oct 2003

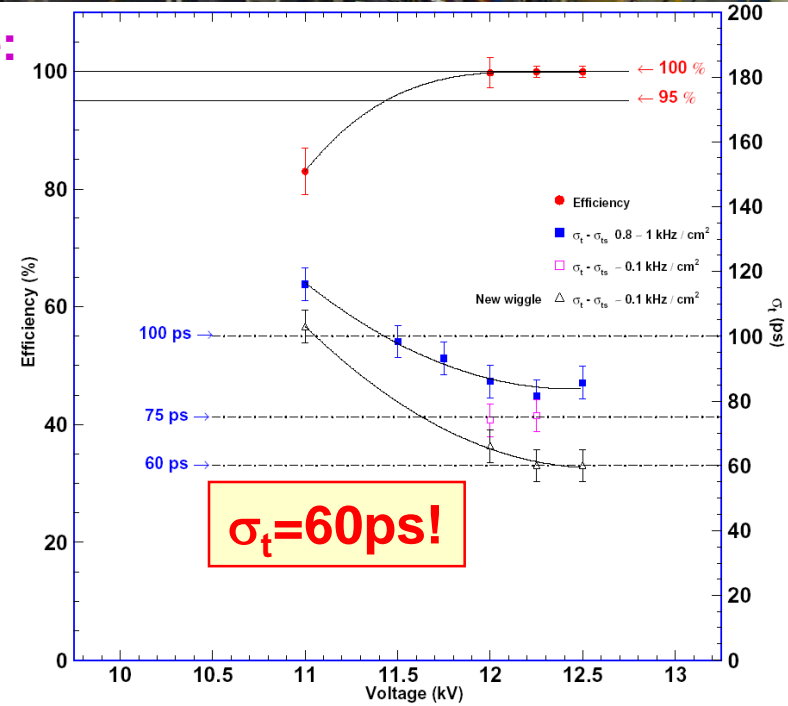


Multi-Gap-Strip-RPC

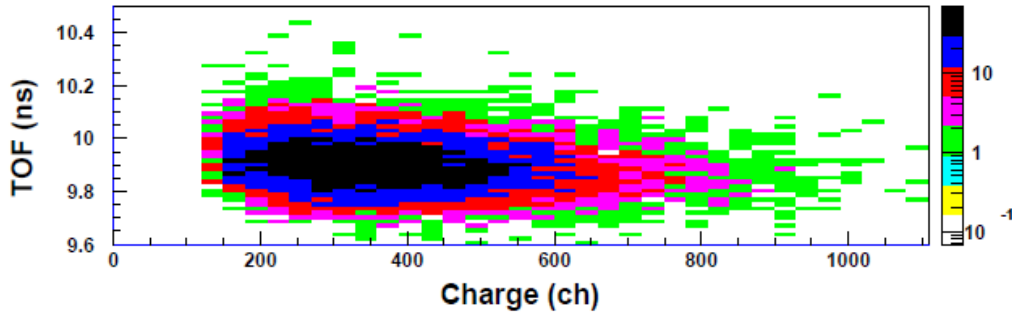
Gap-size: 250-300 μm
High voltage: $\sim 3\text{kV/gap}$
Length: 90 cm
Pitch: 2.54 mm



Performance:

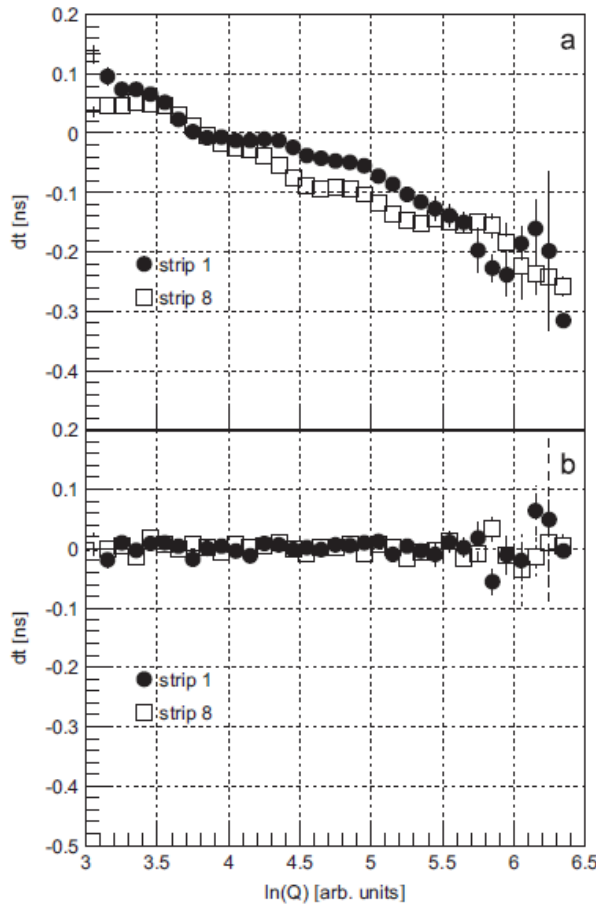


Walk (slewing) correction



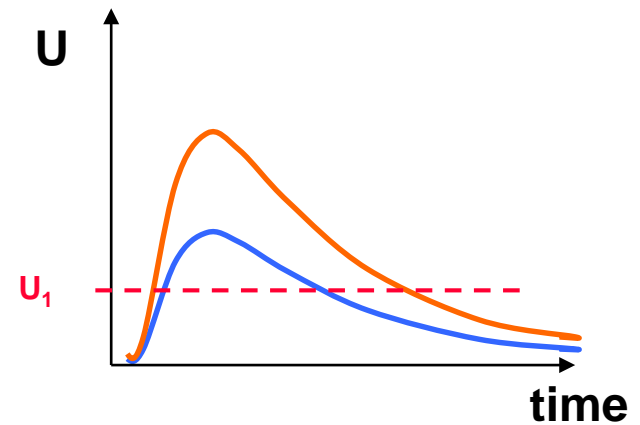
Measured correlation TOF vs. Charge

Mean deviation:
 $t_{\text{meas}} - t_{\text{exp}}$



after correction
 $t_{\text{meas}} - t_{\text{exp}}$

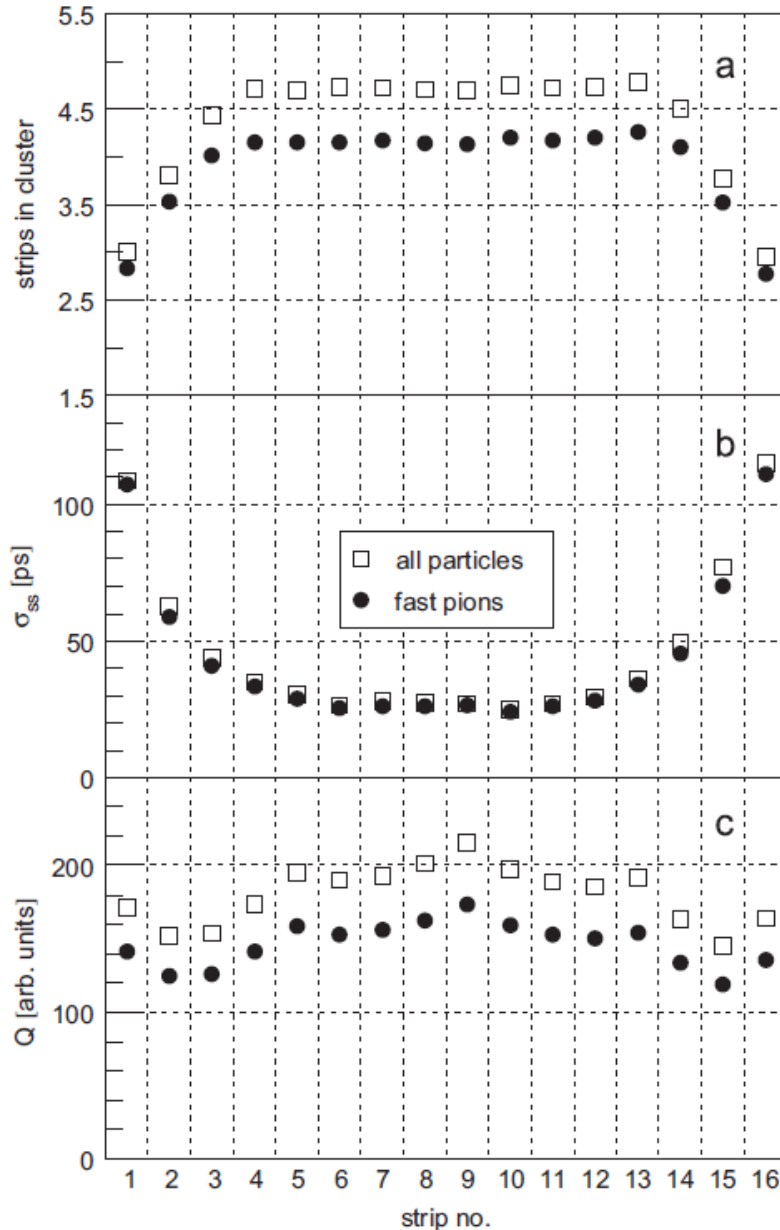
Leading edge discriminator



Corrections done individually
for each strip (~ 2400)

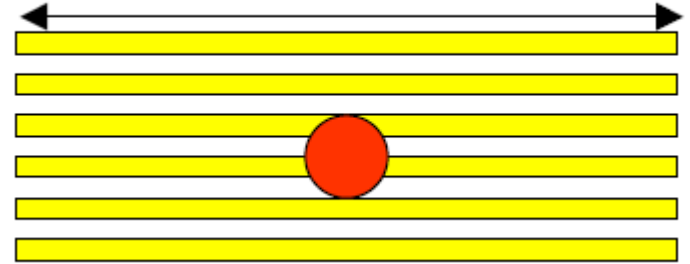
FOPi multi-strip response

M. Kis et al. (FOPi), NIM A 646, 27 (2011)



Number of coincident strips

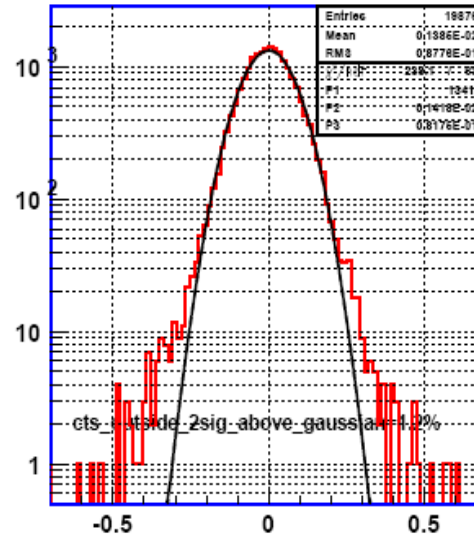
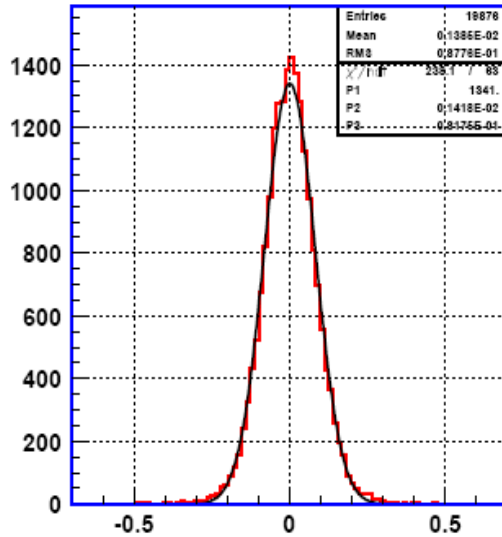
90 cm



RMS of cluster times

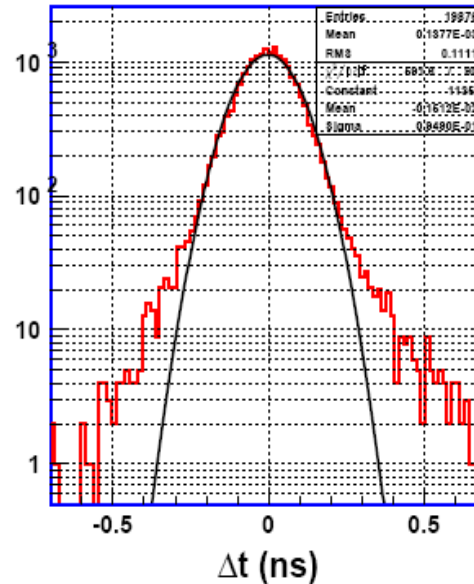
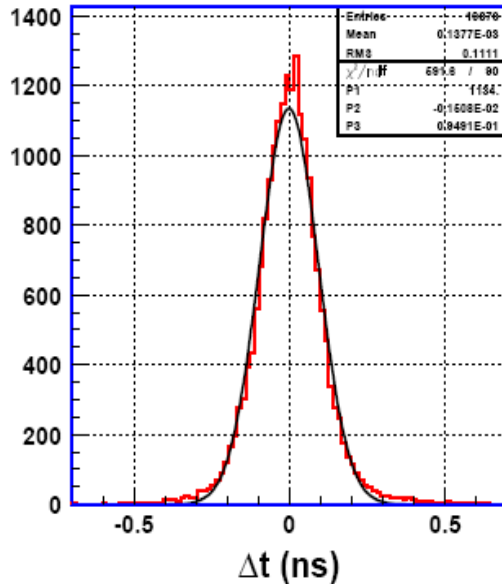
Total charge of cluster

MMRPC timing resolution from RPC-RPC coincidences



RPC against start

$$\sigma_t = 82 \text{ ps}$$



RPC – RPC coincidences

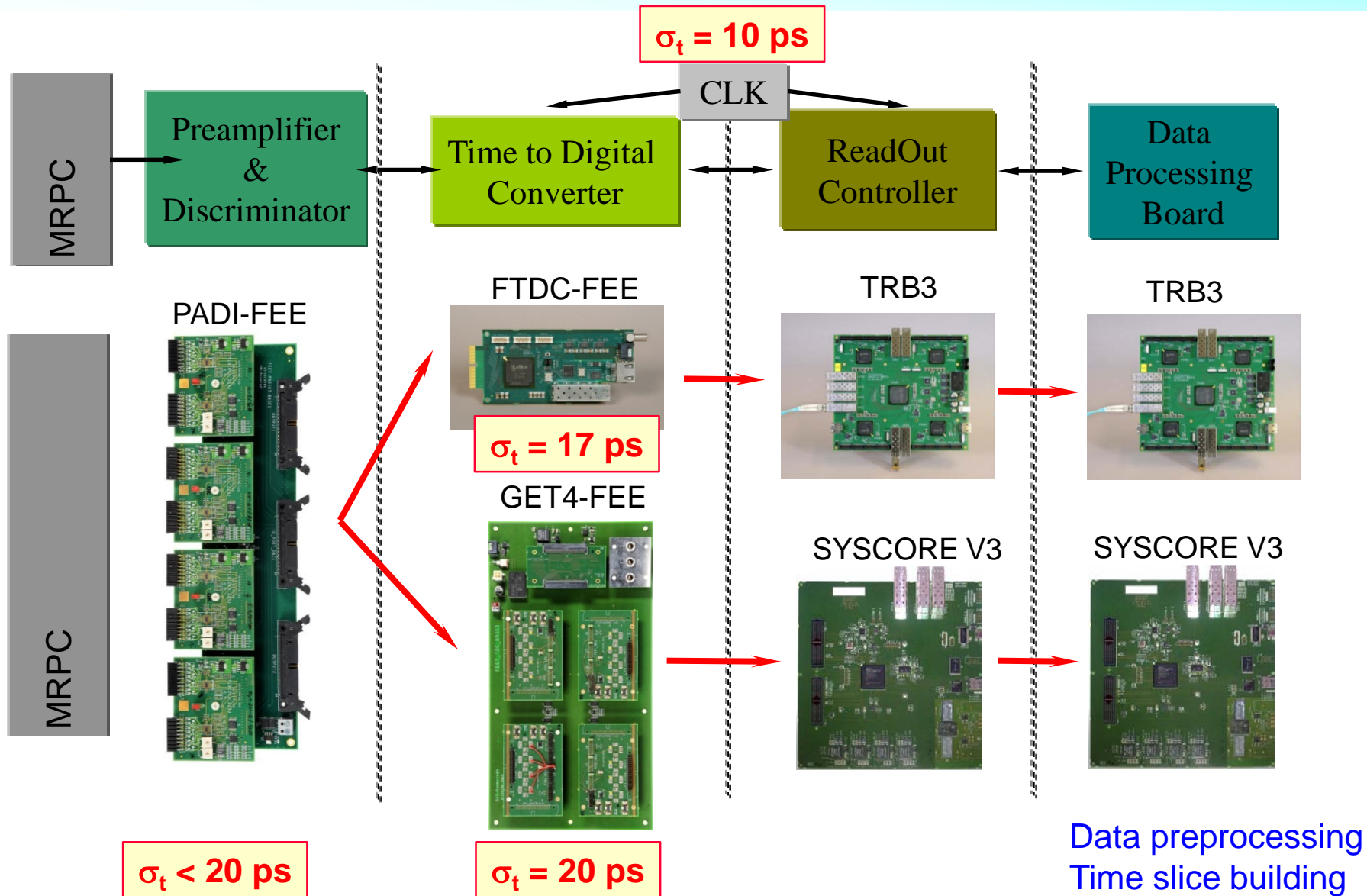
$$\sigma_{\Delta t} = 94.9 \text{ ps}$$

↓

$$\sigma_{\text{RPC}} = 67.1 \text{ ps}$$

(calibration AD-C-F)

CBM – TOF Readout Electronics



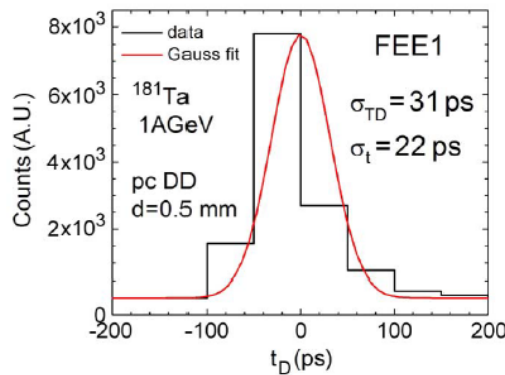
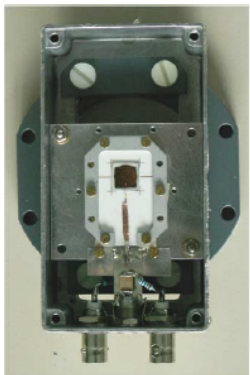
T0 – Beam Counters

Physical Property at 300 K	Diamond	Silicon
band gap [eV]	5.45	1.12
Electron mobility [cm ² /Vs]	2200	1500
Hole mobility [cm ² /Vs]	1600	600
Breakdown field [V/m]	10 ⁷	3x10 ⁵
Resistivity [Ω cm]	>10 ¹³	2.3x10 ⁵
Dielectric constant ε _r	5.7	11.9
Thermal conductivity [W/cm K]	20	1.27
Lattice constant [Å]	3.57	5.43
Energy to remove an atom from the lattice [eV]	80	28
Energy to create an e-h pair [eV]	13	3.6

Favorable material parameter

- mechanical hardness
- high thermal conductivity
- Insensitive for visible light
- No cooling needed
- No p-n junction needed
- Fast signal rise time
- Radiation hardness

Single-crystal CVD diamond plate, max. size: 5x5 mm², d=50,100,200,300μm
 Polycrystalline CVD diamond plate, max. size: 50x50 mm², d=50,100,200,300mm



M. Ciobanu et al.,
 IEEE Transactions of Nuclear Science, 58 (2011) 203

Key issue: fast electronics

$$\sigma_t = \frac{\sigma_{noise}}{\left. \frac{dS}{dt} \right|_{S_{threshold}}} \approx \frac{t_{rise}}{S/N}$$

Fig. 13. The pcDD set used in a ¹⁸¹Ta beam of 1 A GeV (left). The time difference spectrum measured between two identical detectors (right). The time resolution is 22 ps.

Conclusions

Development of particle / photon counters for timing applications is a very active field.

- enabled by fast large bandwidth electronics.
- approaches large scale 50 ps systems.
- 10 – 20 ps achievable for small counters.

Timing Photon Counters

Need: fast scintillator

Table 33.4: Properties of several inorganic crystals. Most of the notation is defined in Sec. 6 of this *Review*.

Parameter:	ρ	MP	X_0^*	R_M^*	dE^*/dx	λ_I^*	τ_{decay}	λ_{max}	n^{\ddagger}	Relative output [†]	Hygroscopic?	$d(\text{LY})/dT$
Units:	g/cm^3	$^{\circ}\text{C}$	cm	cm	MeV/cm	cm	ns	nm				$\%/^{\circ}\text{C}^{\ddagger}$
NaI(Tl)	3.67	651	2.59	4.13	4.8	42.9	245	410	1.85	100	yes	-0.2
BGO	7.13	1050	1.12	2.23	9.0	22.8	300	480	2.15	21	no	-0.9
BaF ₂	4.89	1280	2.03	3.10	6.5	30.7	650 ^s 0.9 ^f	300 ^s 220 ^f	1.50	36 ^s 4.1 ^f	no	-1.9 ^s 0.1 ^f
CsI(Tl)	4.51	621	1.86	3.57	5.6	39.3	1220	550	1.79	165	slight	0.4
CsI(Na)	4.51	621	1.86	3.57	5.6	39.3	690	420	1.84	88	yes	0.4
CsI(pure)	4.51	621	1.86	3.57	5.6	39.3	30 ^s 6 ^f	310	1.95	3.6 ^s 1.1 ^f	slight	-1.4
PbWO ₄	8.30	1123	0.89	2.00	10.1	20.7	30 ^s 10 ^f	425 ^s 420 ^f	2.20	0.3 ^s 0.077 ^f	no	-2.5
LSO(Ce)	7.40	2050	1.14	2.07	9.6	20.9	40	402	1.82	85	no	-0.2
PbF ₂	7.77	824	0.93	2.21	9.4	21.0	-	-	-	Cherenkov	no	-
CeF ₃	6.16	1460	1.70	2.41	8.42	23.2	30	340	1.62	7.3	no	0
LaBr ₃ (Ce)	5.29	783	1.88	2.85	6.90	30.4	20	356	1.9	180	yes	0.2
CeBr ₃	5.23	722	1.96	2.97	6.65	31.5	17	371	1.9	165	yes	-0.1